

Efficient time-dependent vibrational coupled cluster computations with time-dependent basis sets at the two-mode coupling level: full and hybrid TDMVCC[2]

Andreas Buchgraitz Jensen,^{1, a)} Mads Greisen Højlund,¹ Alberto Zocante,² Niels Kristian Madsen,¹ and Ove Christiansen^{1, b)}

¹⁾*Department of Chemistry, Aarhus University,
Langelandsgade 140, DK-8000 Aarhus C, Denmark*

²⁾*Dipartimento di Scienze e Innovazione Tecnologica, Università del Piemonte Orientale (UPO), Via T. Michel 11, 15100 Alessandria, Italy*

(Dated: August 30, 2023)

ABSTRACT

The computation of the nuclear quantum dynamics of molecules is challenging, requiring both accuracy and efficiency to be applicable to systems of interest. Recently, theories have been developed for employing time-dependent basis functions (denoted modals) with vibrational coupled cluster theory (TDMVCC). The TDMVCC method was introduced along with a pilot implementation, which illustrated good accuracy in benchmark computations. In this paper we report an efficient implementation of TDMVCC covering the case where the wave function and Hamiltonian contain up to two-mode couplings. After a careful regrouping of terms, the wave function can be propagated with a cubic computational scaling with respect to the number of degrees of freedom. We discuss the use of a restricted set of active one-mode basis functions for each mode, as well as two interesting limits: i) the use of a full active basis where the variational modal determination amounts essentially to the variational determination of a time-dependent reference state for the cluster expansion; and ii) the use of a single function as active basis for some degrees of freedom. The latter case defines a hybrid TDMVCC/TDH approach which can obtain an even lower computational scaling. The resulting computational scaling for hybrid and full TDMVCC[2] are illustrated for polyaromatic hydrocarbons (PAHs) with up to 264 modes. Finally, computations on the internal vibrational redistribution on benzoic acid (39 modes) are used to show the faster convergence of TDMVCC/TDH hybrid computations towards TDMVCC compared to simple neglect of some degrees of freedom.

^{a)}Electronic mail: buchgraitz@chem.au.dk

^{b)}Electronic mail: ove@chem.au.dk

I. INTRODUCTION

Molecular dynamics research covers a broad spectrum from classical molecular dynamics (MD) approaches to fully quantum descriptions. Classical MD methods have the advantage of being easily applicable to large systems using simple coordinates, but purely classical MD falls short in capturing quantum effects that are crucial at the atomic level. Quantum-classical trajectory methods incorporate quantum corrections and such methods have seen significant progress through the years; see Refs. 1 and 2 and references therein. In this paper we will, however, focus entirely on wave function methods. Quantum dynamical wave function methods are typically computationally expensive, i.e. they often exhibit exponential scaling of the cost with respect to the system size. While this limitation is not universal, many methods struggle to handle systems with numerous coupling terms and can only treat a limited number of degrees of freedom efficiently.

Recently, vibrational coupled cluster (VCC)³ methods have been extended to the time-dependent domain as time-dependent vibrational coupled cluster (TDVCC)^{4,5}, thus offering a new approach for solving the time-dependent Schrödinger equation (TDSE) for molecular motion numerically. Time-dependent coupled cluster methods have previously been discussed in many contexts⁶⁻¹⁰, and there has been considerable recent activity in time-dependent coupled cluster theory for electrons.^{7,11-15} We shall in the remainder of this work focus exclusively on nuclear motion, although a number of formal aspects are similar. TDVCC has demonstrated its potential as an efficient method for simulating time-dependent phenomena with attractive features with respect to accuracy, convergence in configuration space, and separability properties, but it has also certain drawbacks. In the initial formulation it relies on both a time-independent basis set and a time-independent reference state, which restricts the applicability of the method. The use of cluster amplitudes to describe effects that could be captured in a more compact way by time-dependent basis sets and reference states leads to reduced computational efficiency. To address these limitations, the concept of time-dependent vibrational coupled cluster with time-dependent modals (TDMVCC)¹⁶⁻¹⁸ has been proposed even more recently. The term modal refers simply to one-mode basis functions, similar to the single-particle orbital basis of electronic structure theory from which many-particle basis functions are constructed as products. TDMVCC

aims to combine the advantages of TDVCC with the use of a time-dependent adaptive basis in the spirit of the multiconfiguration time-dependent Hartree (MCTDH)^{19,20} method. MCTDH has proven highly successful in describing quantum dynamics by utilizing a small, adaptive active space, providing accurate results at a reasonable computational cost. However, MCTDH still suffers from exponential scaling with the number of modes in the system. While MCTDH offers a fully correlated description, the much simpler time-dependent Hartree (TDH) method amounts to a mean-field treatment of the dynamics. In fact, TDH can be viewed as a limiting case of MCTDH where each mode has only a single active modal. This simplifying circumstance reduces the computational scaling to quadratic for two-body Hamiltonians in an efficient implementation.^{21,22} To overcome the scaling issue of MCTDH, efforts have been made to achieve polynomial scaling by multilayer schemes (ML-MCTDH)^{23–27} or by truncating the configuration space^{28–33}. The latter direction includes methods such as MCTDH[n]³³ and MR-MCTDH[n]³² where the wave function is constructed in terms of excitations from a reference configuration. This approach is similar to how we will truncate the excitation space of TDMVCC in this paper. Other directions include Gaussian-based MCTDH variants (G-MCTDH) and other multi-configurational methods.^{34–47} See also Ref. 40 for a review of multiple spawning methods. TDMVCC seeks to incorporate the benefits of MCTDH and the TDVCC Ansatz. By introducing a small active space of time-dependent basis functions as in MCTDH and leveraging the fast convergence in configuration space offered by the exponentially parameterized VCC methodology, truncated TDMVCC variants present a potential solution to the exponential scaling problem. Still, the development of TDMVCC is in its infancy and much further research is necessary to fully explore its capabilities.

The previous pilot implementation of TDMVCC could not establish the true low-order polynomial computational scaling of TDMVCC methods, as it relied on very general, but exponentially scaling steps. It was made solely with the aim of investigating accuracy and convergence in simple benchmarks. In this paper, we present an efficient implementation of the TDMVCC method covering the case where the wave function and Hamiltonian contain up to two-mode couplings (henceforth denoted TDMVCC[2]). The two-mode coupling case has a manageable number of terms that can be programmed by hand, something that has been utilized in similar papers in time-independent^{48,49} and time-dependent⁴ cases. We

demonstrate how the TDMVCC[2] method can be implemented to efficiently handle many-mode computations with many-term Hamiltonians, achieving a computational scaling of third order with respect to the system size. In particular, we address the challenge of efficiently computing the TDMVCC mean fields. By manually deriving and implementing all the necessary terms, we establish a highly efficient code and lay the groundwork for future general implementations of TDMVCC. In addition, we discuss two interesting limits of using a restricted set of active one-mode basis functions for each mode: i) the use of a full active basis where the variational modal determination amounts essentially to the variational determination of a time-dependent reference state for the cluster expansion; and ii) the use of a single function as active basis for some degrees of freedom. The latter case defines a hybrid TDMVCC/TDH approach, where some modes are treated at the TDH level. This approach can obtain an even lower computational scaling, where the equations of motion (EOMs) for the TDH modes are similar to those of the simple TDH theory, only with some additional mean-field contributions due to the TDMVCC modes. This work thereby initiates a new way of dealing with large systems with different levels of TDMVCC theory.

The structure of the paper is as follows. In Sec. II, we introduce the necessary theory for the TDMVCC method and derive the expressions in a form suitable for efficient implementation. In Sec. III, we present numerical results that highlight the features of the two-mode implementation, including computations on polycyclic aromatic hydrocarbons (PAHs) with up to 264 modes, as well as TDMVCC and TDMVCC/TDH hybrid computations on benzoic acid. Finally, in Sec. IV, we provide a summary of our findings and offer an outlook for future research.

II. THEORY

A. The many-mode second quantization formulation for biorthogonal bases

The TDMVCC method is formulated using the second quantization (SQ) framework introduced in Ref. 50. In an extension to Ref. 50 and following Refs. 16 and 17, we are working in a biorthogonal framework with the main points repeated in this paper for completeness. The biorthogonality is indicated by using \tilde{a}^\dagger and \tilde{b} for creation and annihilation operators, respectively. The tilde is used to denote the time-dependence of the operators.

Relative to the vacuum state, $|\text{vac}\rangle$, single-mode creation and annihilation operators act as,

$$\tilde{a}_{s^m}^{m\dagger} |\text{vac}\rangle = |\tilde{\varphi}_{s^m}^m\rangle, \quad (1)$$

$$\langle \text{vac} | \tilde{b}_{r^m}^m = \langle \tilde{\varphi}_{r^m}^m|. \quad (2)$$

In first quantization coordinate representation, the right-hand sides would be written as $\tilde{\varphi}_{s^m}^m(q_m, t)$ and $\tilde{\varphi}_{r^m}^m(q_m, t)$. The explicit time-dependence will usually be omitted in the following. One-mode basis functions will generally be denoted modals (in analogy to orbitals for electronic structure theory).

To describe the biorthogonality of the basis, we define the commutator relations

$$\left[\tilde{b}_{r^m}^m, \tilde{a}_{s^{m'}}^{m'\dagger} \right] = \delta_{mm'} \delta_{r^m s^{m'}}, \quad \left[\tilde{a}_{r^m}^{m\dagger}, \tilde{a}_{s^{m'}}^{m'\dagger} \right] = \left[\tilde{b}_{r^m}^m, \tilde{b}_{s^{m'}}^m \right] = 0. \quad (3)$$

The time-dependent biorthogonal creation and annihilation operators will be defined through a linear combination of time-independent orthonormal creation ($a_{\alpha^m}^{m\dagger}$) and annihilation ($a_{\alpha^m}^m$) operators with a set of time-dependent expansion coefficients:

$$\tilde{a}_{p^m}^{m\dagger} = \sum_{\alpha^m} a_{\alpha^m}^{m\dagger} U_{\alpha^m p^m}^m, \quad (4)$$

$$\tilde{b}_{p^m}^m = \sum_{\alpha^m} W_{p^m \alpha^m}^m a_{\alpha^m}^m. \quad (5)$$

We use an index convention with Greek letters α^m for the primitive set of time-independent modals and roman letters p^m, q^m, r^m, s^m for generic time-dependent modals. The full set of time-dependent modals is divided into an active set of modals indexed by u^m, v^m, w^m and a set of secondary modals indexed by x^m, y^m . The active set of modals are those actually present in the wave functions. The number of time-independent modals will later be denoted N while the number of time-dependent modals will be denoted A .

The biorthonormality of the time-dependent modals is captured by the modal expansion coefficients,

$$\sum_{\alpha^m} W_{p^m \alpha^m}^m U_{\alpha^m q^m}^m = \delta_{p^m q^m} \quad \Leftrightarrow \quad \mathbf{W}^m \mathbf{U}^m = \mathbf{I}^m, \quad (6)$$

where we have used matrix notation in the latter equation.

From the creation and annihilation operators we define the shift operator as

$$\tilde{E}_{r^m s^m}^m = \tilde{a}_{r^m}^{m\dagger} \tilde{b}_{s^m}^m. \quad (7)$$

This type of operator is used extensively in Sec. IID either as written above in Eq. (7) or as the one-mode excitation and deexcitation operators,

$$\tilde{\tau}_{a^m}^m = \tilde{E}_{a^m i^m}^m, \quad (8)$$

$$\tilde{\tau}_{a^m}^{m\dagger} = \tilde{E}_{i^m a^m}^m. \quad (9)$$

Here, excitation and deexcitation refer to a reference Hartree product which is given as a string of M creation operators acting on the vacuum:

$$|\tilde{\Phi}\rangle = \prod_{m=1}^M \tilde{a}_{i^m}^{m\dagger} |\text{vac}\rangle. \quad (10)$$

Here, M denotes the number of modes. The index i^m is reserved for the occupied active modal of mode m in the reference state while a^m , b^m , c^m denote unoccupied (virtual) active modals.

We will at times use the compound index μ to mean some collection of mode and modal indices defining a general excitation. Other single Hartree product ket or bra states can, for example, be obtained as

$$|\mu\rangle = \tilde{\tau}_{\mu} |\tilde{\Phi}\rangle, \quad (11)$$

$$\langle\mu'| = \langle\tilde{\Phi}'| \tilde{\tau}_{\mu'}^{\dagger}. \quad (12)$$

In addition, we will use the nomenclature that μ_j denotes a j -mode excitation. In our case the two-mode excitations, μ_2 , are of particular interest. Such excitations are constructed as products of one-mode excitations, i.e.

$$\tilde{\tau}_{\mu_2} = \tilde{\tau}_{a^{m_1} a^{m_2}}^{m_1 m_2} = \tilde{E}_{a^{m_1} i^{m_1}}^{m_1} \tilde{E}_{a^{m_2} i^{m_2}}^{m_2}. \quad (13)$$

B. The TDMVCC method

To obtain an approximation to the time-dependent wave function which exactly solves the TDSE in well-defined limits, we employ the TDMVCC method as introduced in Ref. 16. This section will give a brief overview of the general scheme of the method as well as a summary of the important equations one needs to implement.

The TDMVCC bra and ket Ansätze are given as

$$\langle \bar{\Psi}' | = \langle \tilde{\Psi}' | e^{i\epsilon} = \langle \tilde{\Phi}' | (1 + L) e^{-T} e^{i\epsilon}, \quad (14)$$

$$| \bar{\Psi} \rangle = e^{-i\epsilon} | \tilde{\Psi} \rangle = e^{-i\epsilon} e^T | \tilde{\Phi} \rangle, \quad (15)$$

Here, the T and L operators are defined as

$$T = \sum_{\mu} s_{\mu} \tilde{r}_{\mu}, \quad (16)$$

$$L = \sum_{\mu} l_{\mu} \tilde{r}_{\mu}^{\dagger}. \quad (17)$$

Following the time-dependent bivariational principle (TDBVP)^{6,7}, one defines a Lagrangian

$$\mathcal{L} = \langle \bar{\Psi}' | \left(i \frac{\partial}{\partial t} - \hat{H} \right) | \bar{\Psi} \rangle, \quad (18)$$

and solves the corresponding Euler-Lagrange equations (ELEs) for all parameters. Taking biorthogonality constraints into account, one arrives at¹⁶

$$\dot{\epsilon} = \langle \tilde{\Phi}' | (\hat{H} - \hat{g}) | \tilde{\Psi} \rangle, \quad (19)$$

$$\dot{\mathbf{s}} = -i \boldsymbol{\omega}^{\hat{H} - \hat{g}}, \quad (20)$$

$$\dot{\mathbf{l}} = i \boldsymbol{\eta}^{\hat{H} - \hat{g}}, \quad (21)$$

$$i \dot{\mathbf{W}}_A^m = -\tilde{\mathbf{g}}^m \mathbf{W}_A^m - [\boldsymbol{\rho}^m]^{-1} \check{\mathbf{F}}^m \mathbf{Q}^m, \quad (22)$$

$$i \dot{\mathbf{U}}_A^m = \mathbf{U}_A^m \tilde{\mathbf{g}}^m - \mathbf{Q}^m \check{\mathbf{F}}^m [\boldsymbol{\rho}^m]^{-1}. \quad (23)$$

Here, \mathbf{s} and \mathbf{l} are vectors containing the amplitudes, s_{μ} and l_{μ} . Several other definitions are given in Table I.

The projection matrix $\mathbf{Q}^m = \mathbf{1}^m - \mathbf{U}^m \mathbf{W}^m$ plays the role of projecting onto the secondary space. The $\tilde{\mathbf{g}}^m$ matrix, also termed the constraint matrix, is related to the time-derivative of the creation and annihilation operators as

$$\left[\tilde{b}_{u^m}^m, \dot{\tilde{a}}_{v^m}^{m\dagger} \right] = -i \tilde{g}_{u^m v^m}^m, \quad \left[\dot{\tilde{b}}_{u^m}^m, \tilde{a}_{v^m}^{m\dagger} \right] = i \tilde{g}_{u^m v^m}^m. \quad (24)$$

As discussed in Ref. 16, the TDBVP leads to the following $\tilde{\mathbf{g}}^m$ matrix structure:

$$\tilde{\mathbf{g}}^m = \begin{bmatrix} 0 & ({}^d \tilde{\mathbf{g}}^m)^T \\ {}^u \tilde{\mathbf{g}}^m & 0 \end{bmatrix}. \quad (25)$$

Table I: Definition of variables for TDMVCC in the general case and in the specific two-mode case where $T \rightarrow T_2$, $L \rightarrow L_2$, $\mu \rightarrow \mu_2$ and $\hat{H} = \hat{H}_1 + \hat{H}_2$. For the mean-field matrices we have introduced the semi-locked Hamiltonian operators of Eqs. (51, 52, 57–60). The two-mode specific expressions for the \mathbf{u}^m vector, density matrix and the mean-field matrices are also expanded upon in Secs. IID 2, IID 1 and IID 3, respectively.

Symbol	General definition	Two-mode specific expression
$\omega_\mu^{\hat{H}}$	$\langle \mu' e^{-T} \hat{H} e^T \tilde{\Phi} \rangle$	$\langle \mu'_2 \hat{H}_2 + [\hat{H}_1 + \hat{H}_2, T_2] + \frac{1}{2} [[\hat{H}_2, T_2], T_2] \tilde{\Phi} \rangle$
$\eta_\mu^{\hat{H}}$	$\langle \tilde{\Psi}' [\hat{H}, \tilde{\tau}_\mu] \tilde{\Psi} \rangle$	$\langle \tilde{\Phi}' (1 + L_2) ([\hat{H}_1 + \hat{H}_2, \tilde{\tau}_{\mu_2}] + [[\hat{H}_2, \tilde{\tau}_{\mu_2}], T_2]) \tilde{\Phi} \rangle$
$\rho_{w^m v^m}^m$	$\langle \tilde{\Psi}' \tilde{E}_{v^m w^m}^m \tilde{\Psi} \rangle$	$\langle \tilde{\Phi}' (1 + L_2) (\tilde{E}_{v^m w^m}^m + [\tilde{E}_{v^m w^m}^m, T_2]) \tilde{\Phi} \rangle$
$\check{F}_{\alpha^m v^m}^m$	$\langle \tilde{\Psi}' \tilde{a}_{v^m}^{m\dagger} [a_{\alpha^m}^m, \hat{H}] \tilde{\Psi} \rangle$	$[U \check{\mathbf{H}}_1^m \boldsymbol{\rho}^m]_{\alpha^m v^m} + \langle \tilde{\Psi}' \check{H}_{2,(\alpha^m v^m)}^m \tilde{\Psi} \rangle$
$\check{F}'_{v^m \alpha^m}$	$\langle \tilde{\Psi}' [\hat{H}, a_{\alpha^m}^{m\dagger}] \tilde{b}_{v^m}^m \tilde{\Psi} \rangle$	$[\boldsymbol{\rho}^m W \check{\mathbf{H}}_1^m]_{v^m \alpha^m} + \langle \tilde{\Psi}' \check{H}'_{2,(v^m \alpha^m)} \tilde{\Psi} \rangle$
$u_{a^m}^m$	$\check{F}'_{a^m i^m} - \check{F}_{a^m i^m} + \text{more terms}$	$\check{F}'_{a^m i^m} - \check{F}_{a^m i^m}$

The vectors ${}^d \tilde{\mathbf{g}}^m$ and ${}^u \tilde{\mathbf{g}}^m$ are found by solving two sets of linear equations:

$$\mathbf{Z}^m {}^d \tilde{\mathbf{g}}^m = \boldsymbol{\eta}^{\hat{H},m}, \quad (26)$$

$$-(\mathbf{Z}^m)^T {}^u \tilde{\mathbf{g}}^m = \mathbf{u}^m, \quad (27)$$

Here, we have defined $Z_{a^m b^m}^m = \delta_{a^m b^m} \rho_{i^m i^m}^m - \rho_{a^m b^m}^m$. The density matrix $\boldsymbol{\rho}^m$ and the \mathbf{u}^m vector are discussed in detail for the two-mode case in Secs. IID 1 and IID 2, respectively.

The TDMVCC theory reduces to TDVCC with a time-independent basis when \mathbf{W}^m and \mathbf{U}^m are kept time-independent and \mathbf{g}^m consequently zero, as described in Refs. 4 and 5. In particular, the same structure of the EOMs is found for the phase, ϵ , cluster amplitudes, \mathbf{s} , and left amplitudes, \mathbf{l} . A significant difference though is the necessity of the constraint matrix, \mathbf{g}^m , and determining the time-evolving modals which introduces the need for computing mean-field matrices.

If there is no secondary space, i.e. if all modals are active, the equations for $\dot{\mathbf{U}}_A^m$ and $\dot{\mathbf{W}}_A^m$ simplify significantly as the \mathbf{Q}^m matrix becomes the null matrix effectively zeroing the second term in the two EOMs. The first column of the mean-field matrices are still needed for computing the \mathbf{u}^m vector that is used for computing the variationally optimal $\tilde{\mathbf{g}}^m$; Eqs. (26) and (27). In Sec. IID 5 we will discuss specifically this limit we will call the full active basis

(FAB).

C. Polar parameterization of the modals

In Ref. 17 we described how instabilities can occur in the TDMVCC EOMs when employing a secondary modal basis (i.e. when the active basis is not full), and that such instabilities can also occur for other types of wave functions when a biorthogonal basis is used. This phenomenon was analyzed in detail for general bivariational time-dependent wave functions, and it was shown that the issue occurs because the bra and ket modal bases tend to span different spaces when given enough time in a numerical computation. A solution was proposed based on the reparameterization of the modals through polar decomposition. Fully variational EOMs were derived and subsequently modified in order to lock the bra and ket modal bases together such that they span the same space at any given time. This restricted polar representation corresponds to a modal parameterization of the form

$$\mathbf{U}_A^m = \mathbf{V}_A^m \mathbf{P}^m, \quad (28a)$$

$$\mathbf{W}_A^m = (\mathbf{P}^m)^{-1} (\mathbf{V}_A^m)^\dagger, \quad (28b)$$

where \mathbf{V}_A^m is semi-unitary (has orthonormal columns) and \mathbf{P}^m is Hermitian. Eqs. (28) clearly imply that the columns of \mathbf{U}_A^m and \mathbf{W}_A^m span the same space. Although the modified EOMs are not strictly variational, we found an attractive combination of stability and accuracy. The EOMs for the polar modal parameters are given by

$$i\dot{\mathbf{V}}_A^m = \mathbf{V}_A^m \tilde{\mathbf{g}}'^m + \mathbf{Q}'^m \mathbf{X}^m, \quad (29a)$$

$$i\dot{\mathbf{P}}^m = \mathbf{P}^m \tilde{\mathbf{g}}''^m. \quad (29b)$$

The necessary matrices are all calculated from known quantities in a straightforward manner, using \mathbb{H} and \mathbb{A} to denote the Hermitian and anti-Hermitian parts of a matrix:

$$\mathbf{Q}'^m = \mathbf{1} - \mathbf{V}_A^m (\mathbf{V}_A^m)^\dagger, \quad (30a)$$

$$\mathbf{X}^m = \frac{1}{2} (\check{\mathbf{F}}^m (\boldsymbol{\rho}^m)^{-1} (\mathbf{P}^m)^{-1} + (\mathbf{P}^m (\boldsymbol{\rho}^m)^{-1} \check{\mathbf{F}}'^m)^\dagger), \quad (30b)$$

$$\tilde{\mathbf{g}}'^m = \mathbb{H}(\bar{\mathbf{g}}^m) + \mathbf{T}^m (\boldsymbol{\Gamma}^m \circ ((\mathbf{T}^m)^\dagger \mathbb{A}(\bar{\mathbf{g}}^m) \mathbf{T}^m)) (\mathbf{T}^m)^\dagger, \quad (30c)$$

$$\tilde{\mathbf{g}}''^m = \mathbb{A}(\bar{\mathbf{g}}^m) + \mathbf{T}^m (\boldsymbol{\Gamma}^m \circ ((\mathbf{T}^m)^\dagger \mathbb{A}(\bar{\mathbf{g}}^m) \mathbf{T}^m)) (\mathbf{T}^m)^\dagger. \quad (30d)$$

Here, we have diagonalized \mathbf{P}^m as $\mathbf{P}^m = \mathbf{T}\boldsymbol{\epsilon}\mathbf{T}^\dagger$ and defined the auxiliary matrices $\bar{\mathbf{g}}^m$ and $\boldsymbol{\Gamma}^m$ as

$$\bar{\mathbf{g}}^m = \mathbf{P}^m \tilde{\mathbf{g}}^m (\mathbf{P}^m)^{-1}, \quad (31a)$$

$$\gamma_{p^m q^m}^m = \frac{-\epsilon_p^m + \epsilon_q^m}{\epsilon_p^m + \epsilon_q^m}. \quad (31b)$$

The restricted polar representation requires the original \mathbf{g}^m matrices and a few extra steps that scale only linearly with respect to the number of modes. This extra cost can safely be considered negligible. We will accordingly employ the restricted polar representation throughout without further discussion of its computational cost and features.

D. Two-mode TDMVCC implementation

In the two-mode specific case we truncate the cluster expansion to include at most two-mode excitations. As mentioned, one-mode excitations are redundant and can be excluded as derived in Sec. II.C.3 of Ref. 16. This means that unlike in TDVCC[2] (with static modals), we do not need one-mode excitations in TDMVCC[2], since these degrees of freedom are covered by the time-dependent modals. TDMVCC[2] is defined by letting $T \rightarrow T_2$, $L \rightarrow L_2$ and $\mu \rightarrow \mu_2$. In this study we further restrict ourselves to Hamiltonians containing at most two-mode couplings, i.e. $\hat{H} = \hat{H}_1 + \hat{H}_2$, where \hat{H}_j contains only j -mode couplings. To be specific, let us write the cluster operators in detail:

$$T = \sum_{m_1 < m_2} T^{m_1 m_2} = \sum_{\mu_2} s_{\mu_2} \tilde{T}_{\mu_2} = \sum_{m_1 < m_2} \sum_{a^{m_1} a^{m_2}} s_{a^{m_1} a^{m_2}}^{m_1 m_2} \tilde{T}_{a^{m_1} a^{m_2}}^{m_1 m_2}, \quad (32)$$

$$L = \sum_{m_1 < m_2} L^{m_1 m_2} = \sum_{\mu_2} l_{\mu_2} \tilde{T}_{\mu_2}^\dagger = \sum_{m_1 < m_2} \sum_{a^{m_1} a^{m_2}} l_{a^{m_1} a^{m_2}}^{m_1 m_2} \tilde{T}_{a^{m_1} a^{m_2}}^{m_1 m_2 \dagger}. \quad (33)$$

Note that the summations over modes in the T_2 and L_2 operators runs over unique pairs of modes. In many summations later in this paper we will use a notation allowing us to utilize permutation symmetry, i.e. we set $T^{m_1 m_2} = T^{m_2 m_1}$ and $s_{a^{m_1} a^{m_2}}^{m_1 m_2} = s_{a^{m_2} a^{m_1}}^{m_2 m_1}$ and similarly for L . The reasoning is that excitations in two modes m_1 and m_2 commute, as the mode indices are different by definition. We can use this in detailed expressions including commutation,

e.g.

$$\begin{aligned}
[\tilde{E}_{p^m q^m}^m, T] &= \sum_{m_0 > m} [\tilde{E}_{p^m q^m}^m, T^{mm_0}] + \sum_{m_0 < m} [\tilde{E}_{p^m q^m}^m, T^{m_0 m}] \\
&= \sum_{m_0 > m} [\tilde{E}_{p^m q^m}^m, T^{mm_0}] + \sum_{m_0 < m} [\tilde{E}_{p^m q^m}^m, T^{mm_0}] \\
&= \sum_{m_0 \neq m} [\tilde{E}_{p^m q^m}^m, T^{mm_0}] \\
&= \sum_{m_0 \neq m} \sum_{a^m a^{m_0}} s_{a^m a^{m_0}}^{mm_0} [\tilde{E}_{p^m q^m}^m, \tilde{E}_{a^m i^m}^m] \tilde{E}_{a^{m_0} i^{m_0}}^{m_0}.
\end{aligned} \tag{34}$$

We express the Hamiltonian in a sum-of-products (SOP) format with factors containing one-mode operators, \hat{h}^{mO^m} , where the O^m index refers to a specific operator. Correspondingly, we have one-mode integrals of this operator in the time-dependent basis denoted as $\tilde{h}_{p^m q^m}^{mO^m}$. We can write the \hat{H}_1 and \hat{H}_2 operators as

$$\hat{H}_1 = \sum_m \hat{H}_1^m = \sum_m \sum_{O^m} C_{O^m}^m \hat{h}^{mO^m} = \sum_m \sum_{O^m} C_{O^m}^m \sum_{p^m q^m} \tilde{h}_{p^m q^m}^{mO^m} \tilde{E}_{p^m q^m}^m, \tag{35}$$

$$\begin{aligned}
\hat{H}_2 &= \sum_{m < m_0} \hat{H}_2^{mm_0} = \sum_{m < m_0} \sum_{O^m O^{m_0}} C_{O^m O^{m_0}}^{mm_0} \hat{h}^{mO^m} \hat{h}^{m_0 O^{m_0}} \\
&= \sum_{m < m_0} \sum_{O^m O^{m_0}} C_{O^m O^{m_0}}^{mm_0} \sum_{\substack{p^m q^m \\ t^{m_0} u^{m_0}}} \tilde{h}_{p^m q^m}^{mO^m} \tilde{h}_{t^{m_0} u^{m_0}}^{m_0 O^{m_0}} \tilde{E}_{p^m q^m}^m \tilde{E}_{t^{m_0} u^{m_0}}^{m_0}.
\end{aligned} \tag{36}$$

Here, $C_{O^m}^m$ and $C_{O^m O^{m_0}}^{mm_0}$ are possible fitting coefficients.

The two-mode implementation presented in this paper is obtained by explicitly deriving and hand-coding every single non-zero term. The overall idea and implementation follows that of Refs. 4, 48 and 49, but the mean fields contain other types of terms. As the EOMs for the s_{μ_2} and l_{μ_2} amplitudes presented in Sec. II B are equivalent to the ones derived explicitly in Ref. 4 (apart from the lack of the \hat{g} operator), we re-use the $\omega^{\hat{H}}$ and $\eta^{\hat{H}}$ transformers, as well as the phase evaluation algorithm. The only terms that are left for us to implement are thus the constraint contributions, the modal derivatives, and in particular the efficient evaluation of the \mathbf{u}^m vector, the density matrix (ρ^m) and the mean-field matrices ($\check{\mathbf{F}}^m$ and $\check{\mathbf{F}}'^m$). Of these terms, the mean-field matrices are the most complex to evaluate. They contain many demanding terms, and would be strongly time dominating unless care is taken in reducing operation count and scaling by analysis and use of intermediates. Naively, the computation of the mean-field matrices would scale as M^4 , but this can be reduced to M^3 as explored in later sections.

Including only two-mode excitations in the excitation space and in the Hamiltonian greatly reduces the number of terms from thousands to tens. A first indication of this is given later in Tables II and III.

1. The density matrix

We will start out with an explicit derivation of the TDMVCC[2] density matrix, as it showcases general ideas that can be applied to many of the following equations. Starting from the definition of the density matrix, we simply expand the bra and ket states and then apply a Baker-Campbell-Hausdorff (BCH) expansion which terminates after only two terms, because the T and L operators only contain two-mode excitations/deexcitations. This procedure yields

$$\begin{aligned}
\rho_{w^m v^m}^m &= \langle \tilde{\Psi}' | \tilde{E}_{v^m w^m}^m | \tilde{\Psi} \rangle \\
&= \langle \tilde{\Phi}' | (1 + L_2) e^{-T_2} \tilde{E}_{v^m w^m}^m e^{T_2} | \tilde{\Phi} \rangle \\
&= \langle \tilde{\Phi}' | (1 + L_2) (\tilde{E}_{v^m w^m}^m + [\tilde{E}_{v^m w^m}^m, T_2]) | \tilde{\Phi} \rangle \\
&= \delta_{i^m w^m} \delta_{i^m v^m} + \langle \tilde{\Phi}' | L_2 [\tilde{E}_{v^m w^m}^m, T_2] | \tilde{\Phi} \rangle.
\end{aligned} \tag{37}$$

Specifying the modals as either reference or virtual, only four combinations are possible:

1. Passive: $(v^m, w^m) = (i^m, i^m)$
2. Up: $(v^m, w^m) = (a^m, i^m)$
3. Down: $(v^m, w^m) = (i^m, a^m)$
4. Forward: $(v^m, w^m) = (a^m, b^m)$.

It is rather easy to see that the up and down elements vanish as the shift operator becomes either an excitation or deexcitation operator, i.e. $\rho_{a^m i^m}^m = \rho_{i^m a^m}^m = 0$. The remaining cases;

passive and forward give non-zero contributions. The passive indices results in

$$\begin{aligned}
\rho_{i^m i^m}^m &= 1 + \langle \tilde{\Phi}' | L_2 \left[\tilde{E}_{i^m i^m}^m, T_2 \right] | \tilde{\Phi} \rangle \\
&= 1 + \sum_{m_0 \neq m} \sum_{a^m b^{m_0}} s_{a^m b^{m_0}}^{m m_0} \langle \tilde{\Phi}' | L_2 \left[\tilde{E}_{i^m i^m}^m, \tilde{\tau}_{a^m b^{m_0}}^{m m_0} \right] | \tilde{\Phi} \rangle \\
&= 1 - \sum_{m_0 \neq m} \sum_{a^m b^{m_0}} s_{a^m b^{m_0}}^{m m_0} \langle \tilde{\Phi}' | L_2 \tilde{\tau}_{a^m b^{m_0}}^{m m_0} \tilde{E}_{i^m i^m}^m | \tilde{\Phi} \rangle \\
&= 1 - \sum_{m_0 \neq m} \sum_{a^m b^{m_0}} s_{a^m b^{m_0}}^{m m_0} l_{a^m b^{m_0}}^{m m_0}. \tag{38}
\end{aligned}$$

Following the same logic we can get an expression for the forward contribution, where we obtain a sum over matrix products given as

$$\rho_{b^m a^m}^m = \sum_{m_0 \neq m} \sum_{c^{m_0}} s_{b^m c^{m_0}}^{m m_0} l_{a^m c^{m_0}}^{m m_0}. \tag{39}$$

2. The \mathbf{u}^m vector

Another important quantity to compute is the \mathbf{u}^m vector; see Eq. (A29) in Ref. 16. Utilizing the fact that μ is strictly a two-mode excitation (μ_2) simplifies this expression significantly. Equation (A29) reads

$$u_{a^m}^m = \tilde{F}'_{a^m i^m} - \tilde{F}_{a^m i^m}^m + \sum_{\mu} \left(\langle \tilde{\Psi}' | [\tilde{\tau}_{a^m}^{m\dagger}, \tilde{\tau}_{\mu}] | \tilde{\Psi} \rangle (i\dot{s}_{\mu}) + (i\dot{l}_{\mu}) \langle \tilde{\mu}' | e^{-T} \tilde{\tau}_{a^m}^{m\dagger} | \tilde{\Psi} \rangle \right). \tag{40}$$

Assuming that the fully transformed mean-field matrices as well as $\dot{\mathbf{I}}$ and $\dot{\mathbf{s}}$ are calculated and saved elsewhere, we are left with the summation over μ and write this out with explicit two-mode cluster operators as

$$u_{a^m}^m \leftarrow \sum_{\mu_2} \left(\langle \tilde{\Phi}' | (1 + L_2) e^{-T_2} [\tilde{\tau}_{a^m}^{m\dagger}, \tilde{\tau}_{\mu_2}] e^{T_2} | \tilde{\Phi} \rangle (i\dot{s}_{\mu_2}) + (i\dot{l}_{\mu_2}) \langle \tilde{\mu}'_{\mu_2} | e^{-T_2} \tilde{\tau}_{a^m}^{m\dagger} e^{T_2} | \tilde{\Phi} \rangle \right). \tag{41}$$

The two terms are expanded using the BCH expansion and examined one at a time. The BCH expansion in the first term evaluates to

$$e^{-T_2} [\tilde{\tau}_{a^m}^{m\dagger}, \tilde{\tau}_{\mu_2}] e^{T_2} = [\tilde{\tau}_{a^m}^{m\dagger}, \tilde{\tau}_{\mu_2}] + \left[[\tilde{\tau}_{a^m}^{m\dagger}, \tilde{\tau}_{\mu_2}], T_2 \right] + \left[\left[[\tilde{\tau}_{a^m}^{m\dagger}, \tilde{\tau}_{\mu_2}], T_2 \right], T_2 \right]. \tag{42}$$

It is seen that the resulting three terms contains an even number of excitations (2, 4, 6) due to $\tilde{\tau}_{\mu_2}$ and T_2 , and a single deexcitation due to $\tilde{\tau}_{a^m}^{m\dagger}$. In the full expression we also have

the $(1 + L_2)$ term containing 0 and 2 deexcitations. This means that in total we have an even number of excitations (2, 4, 6) and an odd number of deexcitations (1, 3) resulting in orthogonal bra and ket states. The first term in the μ_2 sum in Eq. (40) therefore always contributes 0 to the \mathbf{u}^m vector. The same procedure can be applied to the second term, again resulting in a vanishing contribution

$$\langle \tilde{\mu}'_2 | e^{-T_2} \tilde{\tau}_{a^m}^{m\dagger} e^{T_2} | \tilde{\Phi} \rangle = \langle \tilde{\mu}'_2 | \left(\tilde{\tau}_{a^m}^{m\dagger} + [\tilde{\tau}_{a^m}^{m\dagger}, T_2] + [[\tilde{\tau}_{a^m}^{m\dagger}, T_2], T_2] \right) | \tilde{\Phi} \rangle = 0. \quad (43)$$

Thus, the $u_{a^m}^m$ vector elements for the two-mode couplings case is simply the difference of the first columns in the mean-field matrices, i.e.

$$u_{a^m}^m = \tilde{F}_{a^m i^m}^m - \tilde{F}_{a^m i^m}^m. \quad (44)$$

Again, this encourages an efficient implementation of the mean-field matrices which will be presented in Sec. IID 3.

3. Mean-field equations

As mentioned in Sec. IIB an efficient implementation of the mean-field matrices is key to an efficient implementation of the TDMVCC method. We will thus elaborate on the specifics of the equations for the mean fields in this and the next section. The half-transformed mean fields defined in Ref. 16 are given as

$$\check{F}_{\alpha^m \nu^m}^m = \langle \tilde{\Psi}' | \tilde{a}_{\nu^m}^{m\dagger} [a_{\alpha^m}^m, \hat{H}] | \tilde{\Psi} \rangle, \quad (45)$$

$$\check{F}_{\nu^m \alpha^m}^m = \langle \tilde{\Psi}' | [\hat{H}, a_{\alpha^m}^{m\dagger}] \tilde{b}_{\nu^m}^m | \tilde{\Psi} \rangle. \quad (46)$$

To obtain computationally convenient expressions for the two-mode part we rewrite the primitive creation and annihilation operators in the biorthogonal basis using Eqs. (4), (5) and (6), giving the following two expressions

$$a_{\alpha^m}^m = \sum_{p^m} U_{\alpha^m p^m}^m \tilde{b}_{p^m}^m, \quad (47)$$

$$a_{\alpha^m}^{m\dagger} = \sum_{p^m} \tilde{a}_{p^m}^{m\dagger} W_{p^m \alpha^m}^m. \quad (48)$$

This means that

$$[a_{\alpha^m}^m, \tilde{E}_{p^m q^m}^m] = U_{\alpha^m p^m}^m \tilde{b}_{q^m}^m, \quad (49)$$

$$[\tilde{E}_{p^m q^m}^m, a_{\alpha^m}^{m\dagger}] = W_{q^m \alpha^m}^m \tilde{a}_{p^m}^{m\dagger}. \quad (50)$$

We can therefore rewrite the essential commutator part of the mean-field expressions using

$$\begin{aligned} \check{H}_{(\alpha^m v^m)}^{mO^m} &= \tilde{a}_{v^m}^{m\dagger} [a_{\alpha^m}^m, \hat{h}^{mO^m}] = \tilde{a}_{v^m}^{m\dagger} \sum_{p^m q^m} \tilde{h}_{p^m q^m}^{mO^m} [a_{\alpha^m}^m, \tilde{E}_{p^m q^m}^m] \\ &= \tilde{a}_{v^m}^{m\dagger} \sum_{p^m q^m} \tilde{h}_{p^m q^m}^{mO^m} U_{\alpha^m p^m}^m \tilde{b}_{q^m}^m \\ &= \sum_{q^m} U \check{h}_{\alpha^m q^m}^{mO^m} \tilde{E}_{v^m q^m}^m \end{aligned} \quad (51)$$

$$\check{H}_{(v^m \alpha^m)}^{mO^m} = [\hat{h}^{mO^m}, \tilde{a}_{\alpha^m}^{m\dagger}] a_{v^m}^m = \sum_{p^m} W \check{h}_{p^m \alpha^m}^{mO^m} \tilde{E}_{p^m v^m}^m \quad (52)$$

Here, we have introduced one-mode integrals that are transformed halfway into the primitive basis:

$$U \check{h}_{\alpha^m q^m}^{mO^m} = \sum_{p^m} U_{\alpha^m p^m}^m \tilde{h}_{p^m q^m}^{mO^m}, \quad (53)$$

$$W \check{h}_{v^m \alpha^m}^{mO^m} = \sum_{q^m} W_{q^m \alpha^m}^m \tilde{h}_{p^m q^m}^{mO^m}. \quad (54)$$

Now, if Eqs. (35), (36), (49) and (50) are inserted into Eqs. (45) and (46), we can write the one- and two-mode Hamiltonian contributions to the mean fields as expectation values of effective operators. We thus obtain

$$\check{F}_{\alpha^m v^m}^m = \langle \tilde{\Psi}' | \check{H}_{1,(\alpha^m v^m)}^m | \tilde{\Psi} \rangle + \langle \tilde{\Psi}' | \check{H}_{2,(\alpha^m v^m)}^m | \tilde{\Psi} \rangle, \quad (55)$$

$$\check{F}_{v^m \alpha^m}^m = \langle \tilde{\Psi}' | \check{H}_{1,(v^m \alpha^m)}^m | \tilde{\Psi} \rangle + \langle \tilde{\Psi}' | \check{H}_{2,(v^m \alpha^m)}^m | \tilde{\Psi} \rangle, \quad (56)$$

with the mode-locked operators defined as

$$\check{H}_{1,(\alpha^m v^m)}^m = \sum_{O^m} C_{O^m}^m \check{H}_{(\alpha^m v^m)}^{mO^m}, \quad (57)$$

$$\check{H}_{1,(v^m \alpha^m)}^m = \sum_{O^m} C_{O^m}^m \check{H}_{(v^m \alpha^m)}^{mO^m}, \quad (58)$$

$$\check{H}_{2,(\alpha^m v^m)}^m = \sum_{\substack{m_0 < m \\ m_0 > m}} \sum_{O^m O^{m_0}} C_{O^m O^{m_0}}^{m m_0} \check{H}_{(\alpha^m v^m)}^{mO^m} \tilde{h}^{m_0 O^{m_0}}, \quad (59)$$

$$\check{H}_{2,(v^m \alpha^m)}^m = \sum_{\substack{m_0 < m \\ m_0 > m}} \sum_{O^m O^{m_0}} C_{O^m O^{m_0}}^{m m_0} \check{H}_{(v^m \alpha^m)}^{mO^m} \tilde{h}^{m_0 O^{m_0}}. \quad (60)$$

In accord with Ref. 16, the contributions to the mean fields from \hat{H}_1 can be computed efficiently from the density matrix as

$${}^{1M}\tilde{F}_{\alpha^m v^m}^m = \langle \tilde{\Psi}' | \check{H}_{1,(\alpha^m v^m)}^m | \tilde{\Psi} \rangle = \sum_{O^m} C_{O^m}^m \sum_{w^m} U \check{h}_{\alpha^m w^m}^{m O^m} \rho_{w^m v^m}^m = \left[U \check{\mathbf{H}}_1^m \boldsymbol{\rho}^m \right]_{\alpha^m v^m}, \quad (61)$$

$${}^{1M}\tilde{F}_{v^m \alpha^m}^m = \langle \tilde{\Psi}' | \check{H}_{1,(v^m \alpha^m)}^m | \tilde{\Psi} \rangle = \sum_{O^m} C_{O^m}^m \sum_{w^m} W \check{h}_{w^m \alpha^m}^{m O^m} \rho_{v^m w^m}^m = \left[\boldsymbol{\rho}^m W \check{\mathbf{H}}_1^m \right]_{v^m \alpha^m}. \quad (62)$$

The two-mode contributions to the mean fields can be written as

$${}^{2M}\tilde{F}_{\alpha^m v^m}^m = \sum_{\substack{m_0 < m \\ m_0 > m}} \sum_{O^m O^{m_0}} C_{O^m O^{m_0}}^{m m_0} \sum_{w^m} U \check{h}_{\alpha^m w^m}^{m O^m} \sum_{t^{m_0} u^{m_0}} \tilde{h}_{t^{m_0} u^{m_0}}^{m_0 O^{m_0}} \langle \tilde{\Psi}' | \tilde{E}_{v^m w^m}^m \tilde{E}_{t^{m_0} u^{m_0}}^{m_0} | \tilde{\Psi} \rangle, \quad (63)$$

$${}^{2M}\tilde{F}_{v^m \alpha^m}^m = \sum_{\substack{m_0 < m \\ m_0 > m}} \sum_{O^m O^{m_0}} C_{O^m O^{m_0}}^{m m_0} \sum_{w^m} W \check{h}_{w^m \alpha^m}^{m O^m} \sum_{t^{m_0} u^{m_0}} \tilde{h}_{t^{m_0} u^{m_0}}^{m_0 O^{m_0}} \langle \tilde{\Psi}' | \tilde{E}_{w^m v^m}^m \tilde{E}_{t^{m_0} u^{m_0}}^{m_0} | \tilde{\Psi} \rangle. \quad (64)$$

The two-mode part of the Hamiltonian is much more challenging compared to the one-mode part as we now have two shift operators in our bra-ket expression, giving a set of two-mode density matrix elements. Because of this, non-zero second-order terms are now possible in the BCH expansion. We do not want to compute and store the potentially very large set of two-mode density matrix elements but rather seek to derive all terms and their explicit form. In Tables II and III we have listed all the non-zero contributions to the two mean-field matrices, which can be realized by analyzing Eq. (63) and (64) in the same way as discussed in Sec. IID1. Table IV contains a list of intermediates which are used for the computations.

4. Intermediates for highly efficient mean-field equations

If one were to naively implement the mean-field equations as written in Sec. IID3 the computational cost would scale as M^4 . This would be an order higher than the TDVCC[2] and time-dependent vibrational configuration interaction with singles and doubles (TDVCI[2]) methods (with static modals). Luckily, we can circumvent this issue by the introduction of intermediates. Only a couple of intermediates are strictly necessary for bringing down the scaling exponent, but more have been introduced to bring down the absolute cost as well. We find some intermediates introduced in Refs. 48 and 49, but we will repeat them here for completeness and to account for slight changes in definition and/or notation. All intermediates used have been listed in Table IV with their definition, storage cost and computational

Table II: Contributions to the mean-field matrix $\check{\mathbf{F}}^m$. Intermediates listed are defined in Table IV.

No.	$\check{\mathbf{F}}^m$	BCH order	Contribution	Intermediates
1	$\check{F}_{\alpha^m a^m}^m$	0	$\check{h}_{\alpha^m i^m}^m \check{h}_u^{m_0} L_2 \check{E}_u^m \check{E}_u^{m_0}$	W
2	$\check{F}_{\alpha^m a^m}^m$	1	$\check{h}_{\alpha^m a^m}^m \check{h}_p^{m_0} L_2 \check{E}_f^m \check{E}_p^{m_0} T_2$	Λ
3	$\check{F}_{\alpha^m a^m}^m$	1	$\check{h}_{\alpha^m i^m}^m \check{h}_d^{m_0} L_2 \check{E}_u^m \check{E}_d^{m_0} T_2$	XL
4	$\check{F}_{\alpha^m a^m}^m$	1	$\check{h}_{\alpha^m a^m}^m \check{h}_f^{m_0} L_2 \check{E}_f^m \check{E}_f^{m_0} T_2$	
5	$\check{F}_{\alpha^m i^m}^m$	0	$\check{h}_{\alpha^m i^m}^m \check{h}_p^{m_0} \check{E}_p^m \check{E}_p^{m_0}$	
6	$\check{F}_{\alpha^m i^m}^m$	1	$\check{h}_{\alpha^m a^m}^m \check{h}_d^{m_0} \check{E}_d^m \check{E}_d^{m_0} T_2$	X
7	$\check{F}_{\alpha^m i^m}^m$	1	$-\check{h}_{\alpha^m i^m}^m \check{h}_p^{m_0} L_2 T_2 \check{E}_p^m \check{E}_p^{m_0}$	U
8	$\check{F}_{\alpha^m i^m}^m$	1	$\check{h}_{\alpha^m i^m}^m \check{h}_p^{m_0} L_2 \check{E}_p^m \check{E}_p^{m_0} T_2$	U
9	$\check{F}_{\alpha^m i^m}^m$	1	$\check{h}_{\alpha^m a^m}^m \check{h}_u^{m_0} L_2 \check{E}_d^m \check{E}_u^{m_0} T_2$	WS
10	$\check{F}_{\alpha^m i^m}^m$	1	$\check{h}_{\alpha^m i^m}^m \check{h}_f^{m_0} L_2 \check{E}_p^m \check{E}_f^{m_0} T_2$	V
11	$\check{F}_{\alpha^m i^m}^m$	2	$\check{h}_{\alpha^m a^m}^m \check{h}_d^{m_0} L_2 \check{E}_d^m \check{E}_d^{m_0} T_2 T_2$	Ξ, U, X
12	$\check{F}_{\alpha^m i^m}^m$	2	$-\check{h}_{\alpha^m a^m}^m 2\check{h}_d^{m_0} L_2 T_2 \check{E}_d^m \check{E}_d^{m_0} T_2$	U, X

cost. In this table M^x refers to the scaling regarding the number of modes, A^x denotes the scaling with respect to the size of the active space, and O^x is the scaling with respect to the number of operator terms. Intermediates $(ls)_{a^m a^{m_1}}^{mm_1}$ and U^{mm_0} are of particular importance, as they allow scaling to be reduced from M^4 to M^3 .

We will now look at two intermediates in more detail. The first intermediate, which we will denote by Ξ , arises from contributions 11 and 23. Expanding contribution 11 and 23 from the compact notation in Tables II and III, one obtains several terms among which the following leads to the Ξ intermediate:

$$\sum_{m_1 \neq \{m, m_0\}} \sum_{m_2 \neq \{m, m_0, m_1\}} \sum_{a^{m_1} b^{m_2}} m_0 O^{m_0} X_{a^{m_1}}^{m_1} l_{a^{m_1} b^{m_2}}^{m_1 m_2} S_{a^m b^{m_2}}^{m m_2}. \quad (65)$$

It can be seen there are 4 mode indices (m, m_0, m_1, m_2) giving the M^4 scaling. We introduce the following quantity as an intermediate:

$$(ls)_{a^m a^{m_1}}^{m m_1} = \sum_{m_2 \neq m, m_1} \sum_{b^{m_2}} l_{a^{m_1} b^{m_2}}^{m_1 m_2} S_{a^m b^{m_2}}^{m m_2}. \quad (66)$$

Table III: Contributions to the mean-field matrix $\check{\mathbf{F}}^{m}$. Names for intermediates listed under column 'I' is defined in Table IV.

No. $\check{\mathbf{F}}^{m}$	BCH order	Contribution	I
13 $\check{F}_{i^m \alpha^m}^{m}$	0	$\check{h}_{i^m \alpha^m}^m \check{h}_p^{m_0} \check{E}_p^m \check{E}_p^{m_0}$	
14 $\check{F}_{i^m \alpha^m}^{m}$	0	$\check{h}_{a^m \alpha^m}^m \check{h}_u^{m_0} L_2 \check{E}_u^m \check{E}_u^{m_0}$	W
15 $\check{F}_{i^m \alpha^m}^{m}$	1	$-\check{h}_{i^m \alpha^m}^m \check{h}_p^{m_0} L_2 T_2 \check{E}_p^m \check{E}_p^{m_0}$	U
16 $\check{F}_{i^m \alpha^m}^{m}$	1	$\check{h}_{i^m \alpha^m}^m \check{h}_p^{m_0} L_2 \check{E}_p^m \check{E}_p^{m_0} T_2$	U
17 $\check{F}_{i^m \alpha^m}^{m}$	1	$\check{h}_{a^m \alpha^m}^m \check{h}_d^{m_0} L_2 \check{E}_u^m \check{E}_d^{m_0} T_2$	XL
18 $\check{F}_{i^m \alpha^m}^{m}$	1	$\check{h}_{i^m \alpha^m}^m \check{h}_f^{m_0} L_2 \check{E}_p^m \check{E}_f^{m_0} T_2$	V
19 $\check{F}_{a^m \alpha^m}^{m}$	1	$\check{h}_{i^m \alpha^m}^m \check{h}_d^{m_0} \check{E}_d^m \check{E}_d^{m_0} T_2$	X
20 $\check{F}_{a^m \alpha^m}^{m}$	1	$\check{h}_{a^m \alpha^m}^m \check{h}_p^{m_0} L_2 \check{E}_f^m \check{E}_p^{m_0} T_2$	Λ
21 $\check{F}_{a^m \alpha^m}^{m}$	1	$\check{h}_{i^m \alpha^m}^m \check{h}_u^{m_0} L_2 \check{E}_d^m \check{E}_u^{m_0} T_2$	WS
22 $\check{F}_{a^m \alpha^m}^{m}$	1	$\check{h}_{a^m \alpha^m}^m \check{h}_f^{m_0} L_2 \check{E}_f^m \check{E}_f^{m_0} T_2$	
23 $\check{F}_{a^m \alpha^m}^{m}$	2	$\check{h}_{i^m \alpha^m}^m \check{h}_d^{m_0} L_2 \check{E}_d^m \check{E}_d^{m_0} T_2 T_2$	Ξ, U, X
24 $\check{F}_{a^m \alpha^m}^{m}$	2	$-\check{h}_{i^m \alpha^m}^m 2\check{h}_d^{m_0} L_2 T_2 \check{E}_d^m \check{E}_d^{m_0} T_2$	U, X

Equation (65) can now be written as

$$\sum_{m_1 \neq \{m, m_0\}} \left(\sum_{a^{m_1}}^{m_0 O^{m_0}} X_{a^{m_1}}^{m_1} (l_s)_{a^m a^{m_1}}^{m m_1} \right) - \sum_{b^{m_0}} s_{a^m b^{m_0}}^{m m_0} \left(\sum_{m_1 \neq m, m_0} \sum_{a^{m_1}}^{m_0 O^{m_0}} X_{a^{m_1}}^{m_1} l_{a^{m_1} b^{m_0}}^{m_1 m_0} \right). \quad (67)$$

Only three mode indices are now present (m, m_0, m_1) giving the scaling of M^3 . Of course, it is necessary to compute the intermediates, but this also scales as M^3 requiring two computations with M^3 scaling, which is much more favorable than one computation at M^4 scaling.

The second term contributing to the M^4 scaling stems from contributions 7, 8, 11, 12, 15, 16, 23 and 24 and appears as

$$U^{m m_0} = \sum_{m_1 < m_2 \neq \{m, m_0\}} (LS)^{m_1 m_2} - \sum_{m_1 < m_2} (LS)^{m_1 m_2}. \quad (68)$$

Since all the terms in the first summation is contained in the second, the first term is not computed, and it is a matter of checking when the combinations of mode indices result in something not contained in the first summation and then only compute and subtract these.

Table IV: Intermediates used to reduce computational scaling.

Name	Definition	Storage	Computation
$m_0 O^{m_0} X_a^m$	$\sum_{c^{m_0}} \tilde{h}_{i^{m_0} c^{m_0}}^{m_0 O^{m_0}} s_{a^m c^{m_0}}^{m m_0}$	$M^2 A O$	$M^2 A^2 O$
$m_0 O^{m_0} W_a^m$	$\sum_{c^{m_0}} \tilde{h}_{c^{m_0} i^{m_0}}^{m_0 O^{m_0}} l_{a^m c^{m_0}}^{m m_0}$	$M^2 A O$	$M^2 A^2 O$
$m_0 O^{m_0} (XL)_{a^m}^{m m_0}$	$\sum_{m_1 \neq \{m, m_0\}} \sum_{c^{m_1}} m_0 O^{m_0} X_{c^{m_1}}^{m_1} l_{a^m c^{m_1}}^{m m_1}$	$M^2 A O$	$M^3 A^2 O$
$m_0 O^{m_0} (WS)_{a^m}^{m m_0}$	$\sum_{m_1 \neq \{m, m_0\}} \sum_{c^{m_1}} m_0 O^{m_0} W_{c^{m_1}}^{m_1} s_{a^m c^{m_1}}^{m m_1}$	$M^2 A O$	$M^3 A^2 O$
$(LS)^{m_1 m_2}$	$\sum_{a^{m_1} b^{m_2}} l_{a^{m_1} b^{m_2}}^{m_1 m_2} s_{a^{m_1} b^{m_2}}^{m_1 m_2}$	M^2	$M^2 A^2$
$U^{m m_0}$	$\sum_{m_1 < m_2 \neq \{m, m_0\}} (LS)^{m_1 m_2} - \sum_{m_1 < m_2} (LS)^{m_1 m_2}$	M^2	M^3
$m_0 O^{m_0} V^{m m_0}$	$\sum_{m_1 \neq \{m, m_0\}} \sum_{b^{m_1} c^{m_0} d^{m_0}} l_{b^{m_1} c^{m_0}}^{m_1 m_0} \tilde{h}_{c^{m_0} d^{m_0}}^{m_0 O^{m_0}} s_{b^{m_1} d^{m_0}}^{m_1 m_0}$	$M^2 O$	$M^3 A^3 O$
$\Lambda^{m m_0}$	$\sum_{m_1 \neq \{m, m_0\}} \sum_{c^{m_1}} l_{a^m c^{m_1}}^{m m_1} s_{b^m c^{m_1}}^{m m_1}$	$M^2 A^2$	$M^3 A^3$
$(ls)_{a^m a^{m_1}}^{m m_1}$	$\sum_{m_2 \neq \{m, m_1\}} \sum_{b^{m_2}} s_{a^m b^{m_2}}^{m m_2} l_{a^{m_1} b^{m_2}}^{m_1 m_2}$	$M^2 A^2$	$M^3 A^3$
$m_0 O^{m_0} \Xi_a^{m m_0}$	$\sum_{m_1 \neq \{m, m_0\}} \left(\sum_{a^{m_1}} m_0 O^{m_0} X_{a^{m_1}}^{m_1} (ls)_{a^m a^{m_1}}^{m m_1} \right) - \sum_{b^{m_0}} s_{a^m b^{m_0}}^{m m_0} \left(\sum_{m_1 \neq \{m, m_0\}} \sum_{a^{m_1}} m_0 O^{m_0} X_{a^{m_1}}^{m_1} l_{a^{m_1} b^{m_0}}^{m_1 m_0} \right)$	$M^2 A O$	$M^3 A^2 O$

After introducing these two intermediates (along with the remaining intermediates in Table IV), we can write the final mean-field equations to be computed as follows, with only M^3 scaling cost,

$$\begin{aligned}
 \check{F}_{\alpha^m i^m}^m &= \sum_{\substack{m_0 \leq m \\ m_0 > m}} \sum_{O^m O^{m_0}} C_{O^m O^{m_0}}^{m m_0} \times \\
 &\left\{ U \check{h}_{\alpha^m i^m}^{m O^m} (\tilde{h}_{i^{m_0} i^{m_0}}^{m_0 O^{m_0}} + m_0 O^{m_0} V^{m m_0} + \tilde{h}_{i^{m_0} i^{m_0}}^{m_0 O^{m_0}} U^{m m_0}) \right. \\
 &+ \sum_{a^m} U \check{h}_{\alpha^m a^m}^{m O^m} m_0 O^{m_0} X_{a^m}^m (1 + U^{m m_0}) \\
 &+ \sum_{a^m} U \check{h}_{\alpha^m a^m}^{m O^m} m_0 O^{m_0} (WS)_{a^m}^{m m_0} \\
 &\left. + \sum_{a^m} U \check{h}_{\alpha^m a^m}^{m O^m} m_0 O^{m_0} \Xi_a^{m m_0} \right\} \tag{69}
 \end{aligned}$$

$$\begin{aligned}
\check{F}_{\alpha^m a^m}^m &= \sum_{\substack{m_0 < m \\ m_0 > m}} \sum_{O^m O^{m_0}} C_{O^m O^{m_0}}^{mm_0} \times \\
&\quad \left\{ U \check{h}_{\alpha^m i^m}^{m O^m m_0 O^{m_0}} W_{a^m}^m \right. \\
&\quad + \check{h}_{i^{m_0} i^{m_0}}^{m_0 O^{m_0}} \sum_{b^m} U \check{h}_{\alpha^m b^m}^{m O^m} \Lambda^{mm_0} \\
&\quad + U \check{h}_{\alpha^m i^m}^{m O^m m_0 O^{m_0}} (XL)_{a^m}^{mm_0} \\
&\quad \left. + \sum_{b^m} U \check{h}_{\alpha^m b^m}^{m O^m} \sum_{c^{m_0} d^{m_0}} l_{c^{m_0} a^m}^{m_0 m} \check{h}_{c^{m_0} d^{m_0}}^{m_0 O^{m_0}} S_{d^{m_0} b^m}^{m_0 m} \right\} \quad (70)
\end{aligned}$$

$$\begin{aligned}
\check{F}_{i^m \alpha^m}^{m_0} &= \sum_{\substack{m_0 < m \\ m_0 > m}} \sum_{O^m O^{m_0}} C_{O^m O^{m_0}}^{mm_0} \times \\
&\quad \left\{ W \check{h}_{i^m \alpha^m}^{m O^m} (\check{h}_{i^{m_0} i^{m_0}}^{m_0 O^{m_0}} + m_0 O^{m_0} V^{mm_0} + \check{h}_{i^{m_0} i^{m_0}}^{m_0 O^{m_0}} U^{mm_0}) \right. \\
&\quad + \sum_{a^m} W \check{h}_{a^m \alpha^m}^{m O^m m_0 O^{m_0}} W_{a^m}^m \\
&\quad \left. + \sum_{a^m} W \check{h}_{a^m \alpha^m}^{m O^m m_0 O^{m_0}} (XL)_{a^m}^{mm_0} \right\} \quad (71)
\end{aligned}$$

$$\begin{aligned}
\check{F}_{a^m \alpha^m}^{m_0} &= \sum_{\substack{m_0 < m \\ m_0 > m}} \sum_{O^m O^{m_0}} C_{O^m O^{m_0}}^{mm_0} \times \\
&\quad \left\{ W \check{h}_{i^m \alpha^m}^{m O^m m_0 O^{m_0}} X_{a^m}^m (1 + U^{mm_0}) \right. \\
&\quad + \check{h}_{i^{m_0} i^{m_0}}^{m_0 O^{m_0}} \sum_{b^m} W \check{h}_{b^m \alpha^m}^{m O^m} \Lambda^{mm_0} \\
&\quad + W \check{h}_{i^m \alpha^m}^{m O^m m_0 O^{m_0}} (WS)_{a^m}^{mm_0} \\
&\quad + \sum_{b^m} W \check{h}_{b^m \alpha^m}^{m O^m} \sum_{c^{m_0} d^{m_0}} S_{a^m d^{m_0}}^{mm_0} \check{h}_{c^{m_0} d^{m_0}}^{m_0 O^{m_0}} l_{b^m c^{m_0}}^{mm_0} \\
&\quad \left. + W \check{h}_{i^m \alpha^m}^{m O^m m_0 O^{m_0}} \Xi_{a^m}^{mm_0} \right\} \quad (72)
\end{aligned}$$

5. The full active basis approach

The use of an active space smaller than the full space has been decisive for MCTDH and obviously anticipated to be similarly advantageous for TDMVCC. However, it is of course an additional approximation that may give a basis set truncation error, and it gives rise to additional numerical steps, projections etc. In the FAB limit the time-evolving basis

has solely the purpose of making the reference optimal, which is obviously a theoretically interesting limit. For these reasons we consider the efficient implementation of using the full space as active space to study advantages and disadvantages. In the limit where the primitive and time-dependent modal bases are equal in size, the EOMs simplify significantly, and we only need to compute the parts of the mean-field matrices necessary for computing the \mathbf{u}^m vector. We see in Eq. (44) that this is simply the first column of both the matrices. Expanding the right-hand side of Eq. (112) from Ref. 16,

$$\tilde{F}'_{v^m w^m} - \tilde{F}^m_{v^m w^m} = \langle \tilde{\Psi}' | [\hat{H}, \tilde{E}^m_{w^m v^m}] | \tilde{\Psi} \rangle, \quad (73)$$

as was done in the previous sections results in terms with structure similar to the ones in Eq. (69) and (71), but with fully transformed mean-field matrices rather than half-transformed ones. These two approaches are of course equivalent in the limit of no secondary modal space, but the implementation differs a bit as new efficient intermediates/transformations might become available.

Initially we had hoped for a very fast specialized implementation of this limit, but despite the apparent simplicity of the \mathbf{u}^m vector equations, many expensive terms remain to be computed, and the approach still scales as M^3 .

E. Hybrid TDMVCC/TDH scheme

In this section we present a computational scheme introduced for obtaining an important computational limit which opens up for efficient calculations of large systems. The idea is to apply TDMVCC in the usual way for a selected set of important modes and then only have a single active time-dependent modal for the rest. Thus, we restrict these modes to stay in the reference modal. In this way we obtain a TDMVCC/TDH hybrid scheme where we do not ignore less important modes, as may be a more standard approach. Instead, they are included in a simplified way which makes the computations significantly faster compared to TDMVCC[2]. We denote the modes with the simplified treatment as TDH modes but emphasize that their mean fields will be different from the pure TDH mean fields due to the TDMVCC modes. Thus, one can state that the ket state of the system can be written like

$$|\bar{\Psi}\rangle = e^{-i\epsilon} e^{T^{\text{TDMVCC}}} \prod_{m \in \text{MC}^{\text{TDMVCC}}} \tilde{a}_{i_m}^{m\dagger} \prod_{m \in \text{MC}^{\text{TDH}}} \tilde{a}_{i_m}^{m\dagger} |\text{vac}\rangle \quad (74)$$

The speedup achieved by TDMVCC/TDH is seen by the fact that we can skip certain parts of the calculations involved in solving the EOMs as these TDH modes do not have any virtual modals. For example, we see this effect in the density matrices and the mean-field matrices. The density matrix for a TDH mode reduces to a 1-by-1 matrix with the element 1, as can be seen in Eqs. (38) and (39). The mean-field matrices for the TDH modes reduce to a vector with very few contributions as seen in Eqs. (69) and (71), where the intermediates with a virtual modal index does not contribute.

This approach will be explored further with numerical results in Sec. III C where we utilize it to do computations on a 39-mode potential-energy surface (PES) (coupled at the two-mode level) describing benzoic acid. We will also denote this method as TDMVCC[2|X] where the X denotes the number of modes propagated at the TDMVCC level. The X notation will be used both with absolute numbers, but also with relative quantities indicating a certain percentage of the systems modes which have been propagated at the TDMVCC level. We note that TDMVCC[2|0] will occasionally be named the TDH limit.

III. NUMERICAL RESULTS

The described methods have been implemented in the Molecular Interactions, Dynamics And Simulations Chemistry Program Package (MidasCpp)⁵¹. All computational results presented in the following have been obtained with this implementation.

We will henceforth use the following nomenclature for the three TDMVCC[2] schemes that are considered in this paper: i) hybrid TDMVCC[2] (or TDMVCC[2|X]) denotes the scheme where only a subset of modes is treated at the TDMVCC level; ii) FAB TDMVCC[2] denotes the implementation that has been optimized to run with an equal number of time-dependent and time-independent modals ($A = N$); and iii) TDMVCC[2] (with no further qualifiers) denotes the basic scheme where all modes are treated at the TDMVCC level and where the optimized FAB implementation is not used (even if $A = N$).

A. Mode scaling

Theoretically we found the scaling of the mean fields with respect to the number of modes in the system to be M^3 . The scaling of the implementation of the mean fields computation

has been tested with calculations on 12 PAHs systems with the number of modes ranging from 102 to 192 using pre-computed two-mode PESs^{22,48}. To get representative numbers, we have averaged over 96 evaluations of the mean-field matrices. A b-spline basis was used as the primitive basis with bounds at the 10th classical turning point. For the modals we used the 5 lowest-lying VSCF modals as our stationary basis and then 5 time-dependent modals for Fig. 1, which is sufficient for investigating the scaling of the method with respect the number of modes. The PESs have a relatively large number of terms (in the range 59,000 to 122,000) and are thus representative for real PESs. Obviously, absolute timings would be even more favorable with simple few-term model potentials.

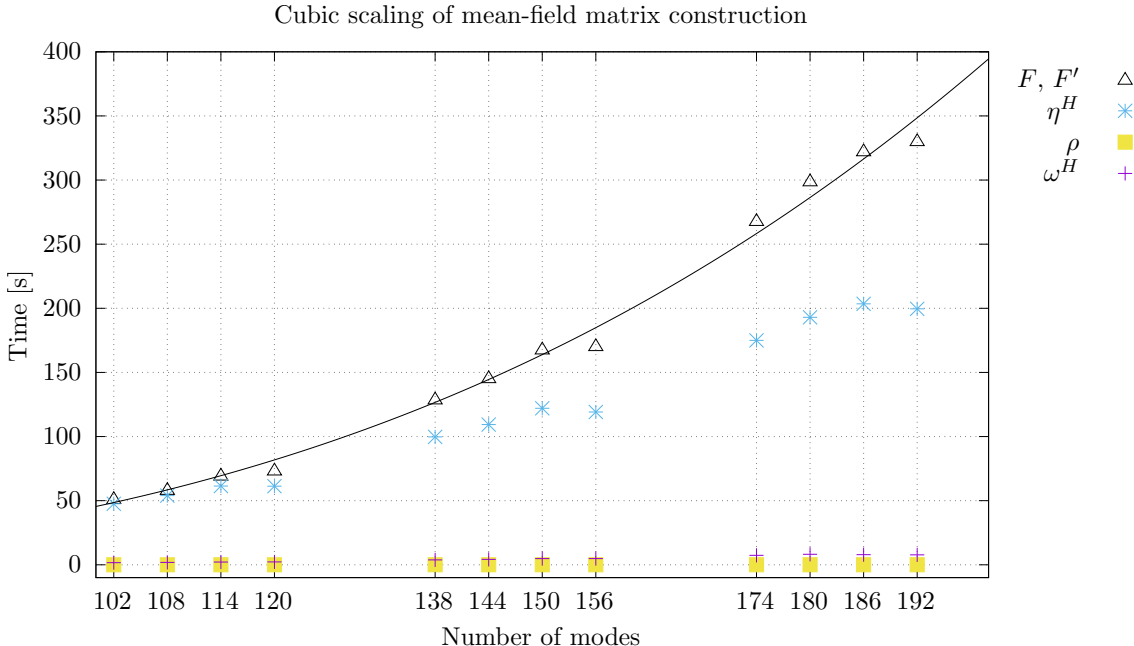


Figure 1: Mode-scaling of the TDMVCC[2] code. The time for computing mean fields follows the theoretical M^3 scaling (black line) quite well. The density matrices are very cheap, as expected. The timings for the vectors $\omega^{\hat{H}}$ and $\eta^{\hat{H}}$ are also shown for absolute timing perspective.

In Fig. 1 the computational times for different part of the TDMVCC method has been plotted. The timings for the $\omega^{\hat{H}}$ and $\eta^{\hat{H}}$ vectors (Refs. 48 and 49) have also been plotted to give a sense of absolute times.

From Fig. 1 we see that a theoretical scaling proportional to M^3 fits rather nicely with

the data for the computation of the total mean-field matrices. We see that the mean-field computations are the major computational task even after our significant optimizations.

In Fig. 2 we show the scaling of four different computational schemes for TDMVCC and for comparison two different versions of TDH. For TDMVCC we show the approach where all modes are propagated at the TDMVCC level, two different hybrid approaches where i) a fixed number of 10 modes are propagated at the TDMVCC level while the rest are kept at the TDH level; ii) 15% percent of the modes propagated at the TDMVCC level; and iii) the limit where all modes are propagated at the TDH level. These results are also run on PAH systems with a range of sizes. Note that the PESs for these timings have been trimmed, keeping only the five lowest-order coupling terms, so that the number of coupling terms are the same for each mode combination (MC). This was done as the number of coupling terms in the PESs do not increase as a simple polynomial as a function of the number of modes, giving spurious fitting for the results shown in Fig. 2. From Fig. 2 we see that the TDMVCC[2|X] scheme is computationally very attractive, as the computational times of the TDMVCC method can be significantly reduced if the important dynamics is located to a small subset of modes. This is especially true if the number of dynamically important modes does not change with respect to the system size. It can be seen that the TDMVCC[2|10] method scales as M^2 just as the TDH method. That is, the 10 modes propagated at the TDMVCC level simply result in a prefactor. If the number of dynamically important modes is not independent on the system size, but still located to a subset of the total modes, we end up with the M^3 scaling, as the number of modes propagated at the TDMVCC level increases. Importantly, this is at a significantly reduced cost compared to propagating all modes at the TDMVCC level.

In the limit where all modes are propagated at the TDH level, we see, despite a lot of logical TDMVCC overhead, that the implementation recovers the M^2 scaling of TDH²¹. The explicit TDH code clearly runs faster still, with the exponentially parameterized TDH as the clear winner. It is an opportunity for future research to implement TDMVCC[2] with exponentially parameterized modals¹⁸ and recover this efficiency gain. However, very large systems and small TDMVCC[2] domains must be considered for this additional gain to be significant.

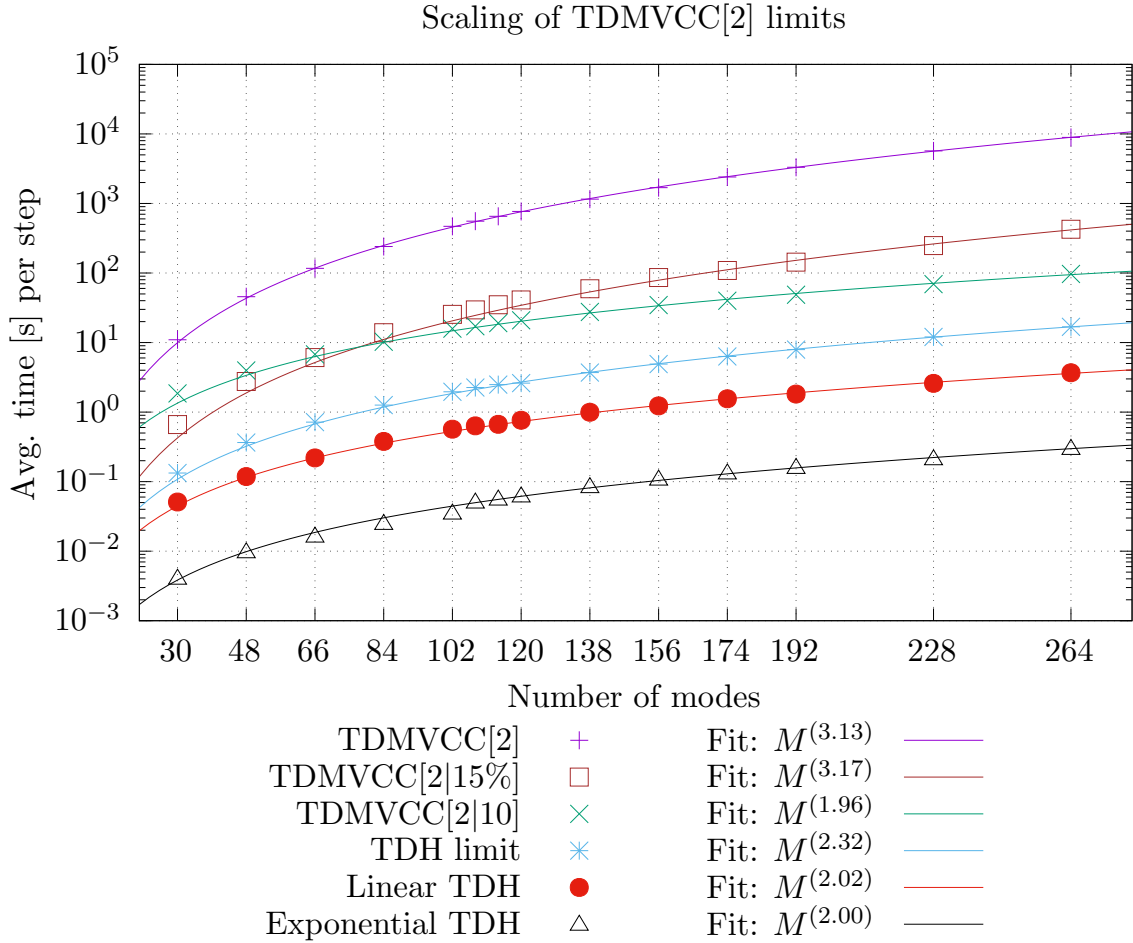


Figure 2: Scaling of TDMVCC[2] and several limiting methods. The two data points between 102 and 120 correspond to 108 and 114 modes. TDMVCC[2|10] and TDMVCC[2|15%] signify that 10 modes or 15% of the modes, respectively, are treated at the TDMVCC level. The remaining modes are propagated at the TDH level.

B. Basis size scaling

Here we investigate the scaling of the method with respect to the basis set size. The setup is very similar to the above computations, we have here limited the computations to PAH systems with 48, 66 and 84 modes, and we only look at the timings for constructing the mean fields as these are the most important factors as shown in Fig. 1. The basis scaling results have been plotted in Fig. 3. For TDMVCC[2] we have fixed $N = 50$ and then varied A . Additionally, we have plotted the same results obtained from a FAB computation

($N = A \leq 50$).

For basis sets larger than 10 we see a reasonable fit to roughly A^3 . This meets our expectations since there are several terms scaling as $M^3 A^3$ as listed in table IV.

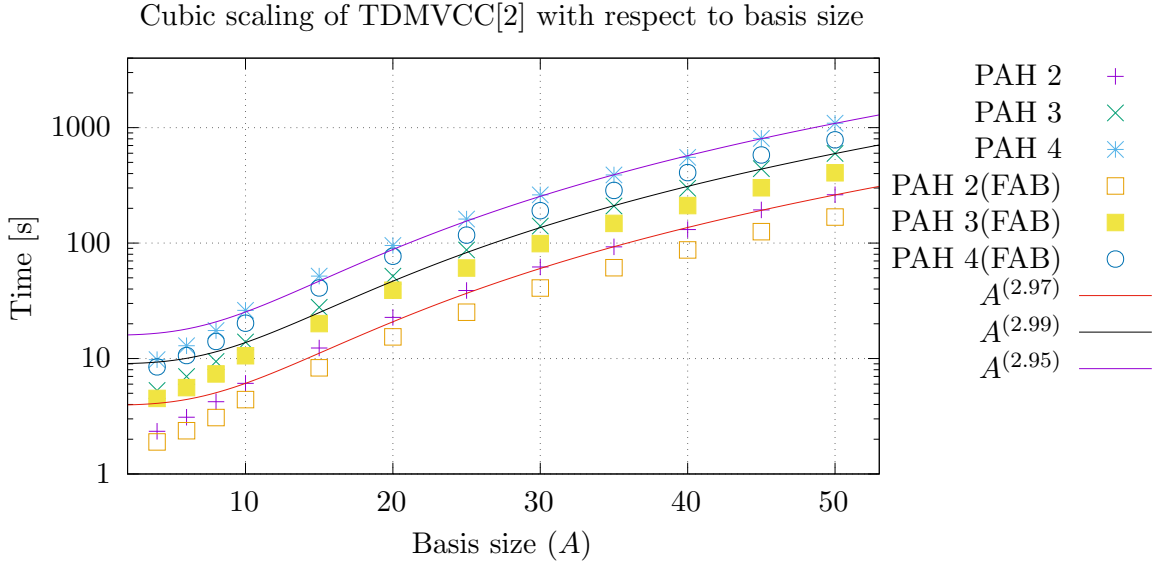


Figure 3: Scaling of TDMVCC[2] with respect to the size of the time-dependent active basis (A). For the TDMVCC[2] implementation, A is varied with $N = 50$ fixed. For the FAB implementation, $A = N \leq 50$ is varied.

In the FAB ($A = N$) limit we see a decrease in computing time. We found the computing time for the TDMVCC[2] implementation to be 1.2–1.6 times slower than the specialized FAB implementation, depending on the system size and the basis size (large basis sets gave larger difference while large systems gave a smaller difference). One of course has to hold this up against the quality of the result: The FAB implementation can of course only be used in the $N = A$ limit, which often yields poor results for realistic values of N . Furthermore, an important point of TDMVCC is that it is not necessary to use $N = A$ to obtain good results and often N can be significantly larger than A . Therefore, the FAB option is mainly of interest from a theoretical point of view. We foresee that the restricted polar parameterization in combination with a small active space will be used in applications.

C. IVR for Benzoic acid

To explore further the numerical behavior of TDMVCC[2] and the quality of the TD-MVCC[2|X] method we present some results on the benzoic acid molecule (39 modes). The PES was obtained using the adaptive density-guided approach (ADGA)⁵² procedure in MidasCpp⁵¹ and the GFN2-xTB method⁵³ in the xTB program for computing cheap single points in these exploratory computations. ADGA settings are given in the supporting information and the final PES has 35,956 terms. The dynamics of the benzoic acid molecule is initialized by using a VSCF state with the mode describing the acid O–H stretch in the first excited state (described by the $v = 1$ modal) computed on an uncoupled PES and then letting this state relax in the coupled PES.

In Fig. 4 the expectation value of the displacement coordinate describing the O–H stretch in the acid group (Q_{38}) is plotted as a function of time. Coordinates Q_{32} and Q_{22} are also shown for comparison. As a reference method we use TDMVCC[2|39] (also simply named TDMVCC[2]) where all modes are described at the coupled cluster level. Each mode has an active basis of four time-dependent modals. We compare the reference calculation with linear TDH and with the hybrid TDMVCC[2|X] method with $X = 8, 13, 18$. The modes to be propagated at the TDMVCC[2] level were chosen by visual inspection (modes dominated by motion localized in the acid group were prioritized). A table is given in the supporting information listing the specific modes used in the different hybrid schemes. Expectation values are generally defined as $\langle \Lambda | \hat{O} | CC \rangle$ for an operator \hat{O} . However, for the simple case of a one-mode operator \hat{O}^m this expression specializes to $\sum_{r^m s^m} \tilde{O}_{r^m s^m}^m \rho_{s^m r^m}^m$, which adds no significant additional cost to the computations.

It is clear that increasing X ensures that the expectation values converge towards the TDMVCC[2] limit, where all modes are treated at the coupled cluster level. We also note that if one wants to do computations on a very large system the computational cost can be significantly reduced by the hybrid approach, and the results are qualitatively very similar. Another observation is that the hybrid approach is much better than TDH.

To show that the hybrid method is favorable compared to a computation with frozen modes (i.e. a computation in reduced dimensionality), we have performed a number of calculations where the less important modes have been frozen completely instead of being

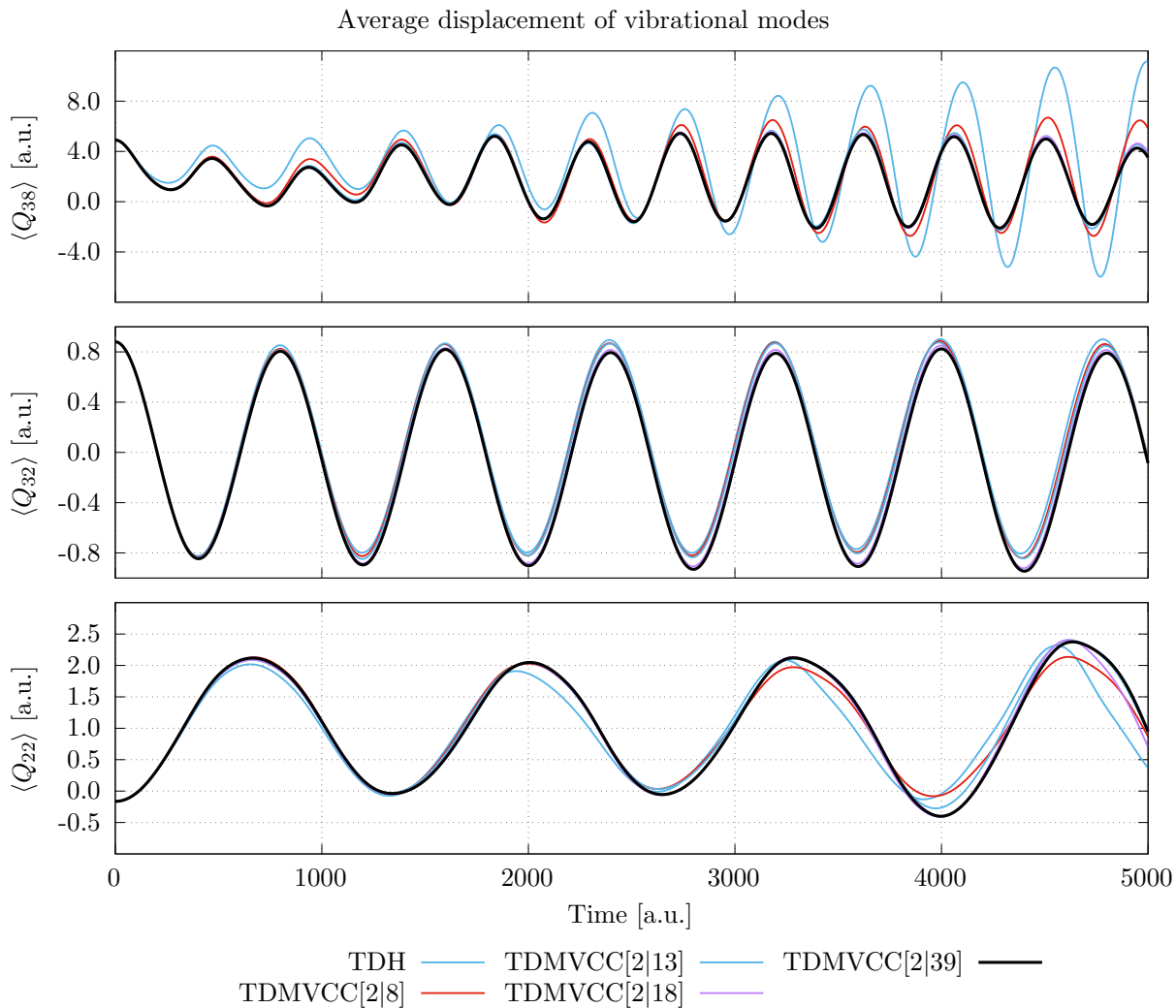


Figure 4: Position expectation values for three coordinates of the benzoic acid molecule. Q_{38} describes the O–H stretch. Q_{32} describes the C=O stretch. Q_{22} describes the in-plane bending mode of the O–H group. The TDMVCC[2|39] computation corresponds simply to TDMVCC[2], i.e. all modes are included as TDMVCC modes.

included as TDH modes. The computational settings are identical to those in Fig. 4 and the results are shown in Fig. 5. We now only show the results for the O–H stretch (Q_{38}) and only the last 1000 time units to easier distinguish between the results. It is seen that both schemes converges towards the TDMVCC[2] results, but that the hybrid schemes does so with a lower number of TDMVCC modes.

Results for the hybrid TDMVCC[2|X] approach are clearly better, but this of course

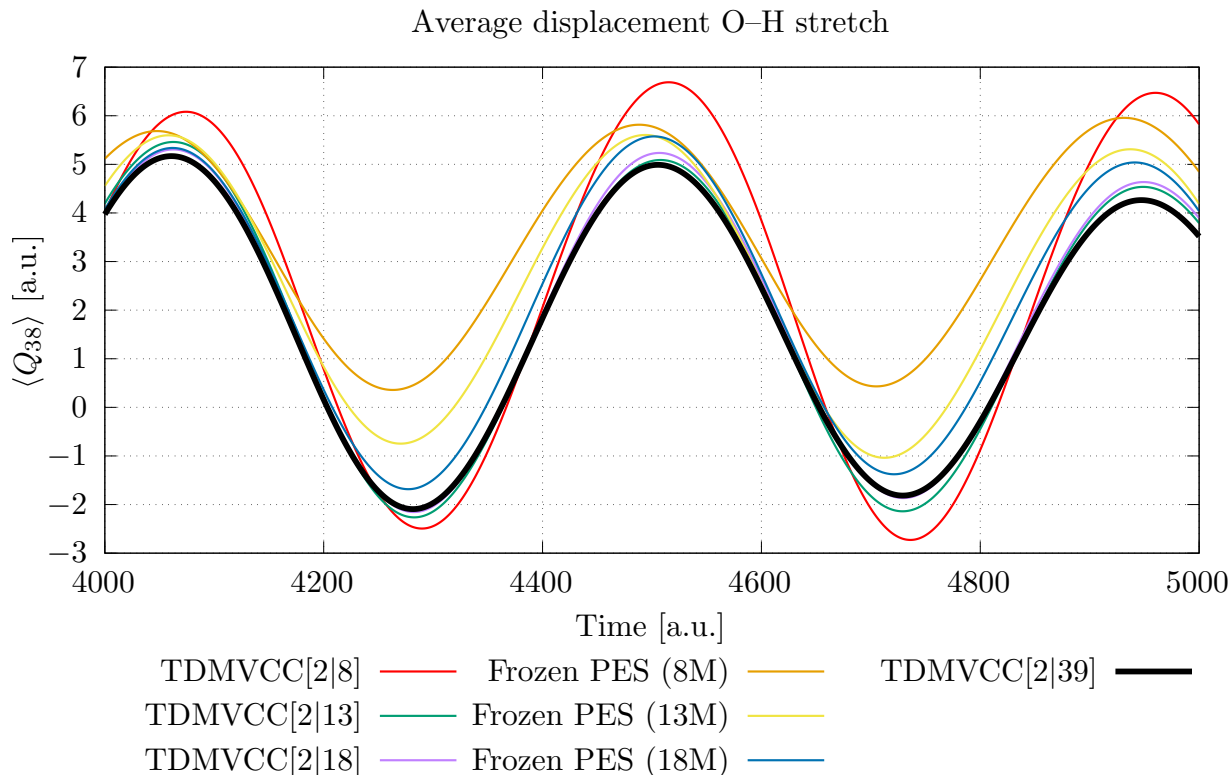


Figure 5: Comparison of the hybrid TDMVCC[2|X] method and reduced dimension PESs for the benzoic acid molecule. The TDMVCC[2|39] computation corresponds simply to TDMVCC[2], i.e. all modes are included as TDMVCC modes.

comes with a more time-consuming calculation. In Table V the approximate timings for several computations shown in Figs. 4 and 5 are listed. The propagation time is 5000 a.u. corresponding to about 120 femtoseconds. So far the implementation only allows for serial calculations, which is an obvious area of improvement for future work.

IV. SUMMARY AND OUTLOOK

This work presents the first efficient implementation of the TDMVCC method. Focusing on the two-mode coupling level, all detailed equations were derived and implemented by hand. We showed that the computational cost of TDMVCC[2] can be reduced to cubic scaling with respect to the number of degrees of freedom by introducing appropriate intermediates. Specializations were made, allowing efficient and flexible usage of both full active basis sets

Table V: Absolute timings of computations presented in Figs. 4 and 5.

Calculation name	Time
TDH:	2 hours
Frozen PES (8M):	1.7 hours
Frozen PES (13M):	6 hours
Frozen PES (18M):	15 hours
TDMVCC[2 8]:	17 hours
TDMVCC[2 13]:	1.4 days
TDMVCC[2 18]:	1.8 days
TDMVCC[2 39]:	7.5 days

and basis sets limited to only a few active basis function per mode. The latter allows for a hybrid TDMVCC/TDH approach that has an even lower quadratic computational scaling as long as the set of TDMVCC modes is kept constant and only the number of TDH modes is extended. The resulting low order scaling was illustrated for PAHs with up to 264 modes, and the gain of TDMVCC/TDH hybrid computations compared to simply freezing some degrees of freedom was illustrated in computations on a 39-mode benzoic acid PES.

The ability to perform these high-dimensional computations shows how TDMVCC may open for accurate quantum dynamical studies on systems that were previously out of reach. The hybrid methods introduced further opens a new line of research where TDMVCC computations can be tailored to balance accuracy, efficiency, and feasibility in quantum dynamical computations.

The work presented here is only the first step in making TDMVCC more generally applicable. In many cases the present two-mode version will not be sufficiently accurate, and higher-level TDMVCC and higher-level couplings in the Hamiltonian will be important. This includes flexible multi-reference schemes along the lines of recent work on MR-MCTDH[n]³². Implementing such higher-level TDMVCC methods must generally be considered as a very hard problem as higher-order TDMVCC methods with higher-order Hamiltonians include numerous terms (on the order of many thousands)⁵. For TDVCC (with static modals), it has been possible to make a general implementation⁵ with well-defined low-order polynomial

scaling of the computational effort by utilizing existing machinery for automatic derivation, analysis and computation of all terms that appear in the equations. However, TDMVCC contains new types of terms (particularly in the mean fields) that fall outside the scope of our current code base. The present work has shown that it is possible and important to construct certain appropriate intermediates to obtain low-order computational scaling. This work therefore paves the way for and encourages the laborious work on general machinery for implementing general order TDMVCC.

SUPPLEMENTARY MATERIAL

The supplementary material contains information regarding the ADGA computations performed for obtaining the benzoic acid PES used in Sec. III. It also contains an overview of all modes in the benzoic acid molecule, their harmonic frequencies, and whether they are treated at the TDMVCC or the TDH level in hybrid computations.

ACKNOWLEDGEMENTS

O.C. acknowledges support from the Independent Research Fund Denmark through grant number 1026-00122B. All calculations were performed on the high performance computing cluster of the Center for Scientific Computing Aarhus. This work was supported by the Danish National Research Foundation through the Center of Excellence for Chemistry of Clouds (Grant Agreement No: D NRF172).

The authors thank Jonas Elm and the Independent Research Fund Denmark for financial support via grant number 9064-00001B.

AUTHOR DECLARATIONS

Conflict of interest

The authors have no conflicts to disclose.

Author contributions

Andreas Buchgraitz Jensen: Conceptualization (equal); Data curation (lead); Formal analysis (equal); Investigation (lead); Software (lead); Visualization (lead); Writing/Original Draft Preparation (equal); Writing/Review & Editing (equal). **Mads Greisen Højlund:** Conceptualization (equal); Formal analysis (equal); Writing/Original Draft Preparation (equal); Writing/Review & Editing (equal). **Alberto Zocante:** Conceptualization (equal); Formal analysis (equal); Writing/Original Draft Preparation (supporting); Writing/Review & Editing (equal). **Niels Kristian Madsen:** Conceptualization (equal); Formal analysis (equal); Software (supporting); Writing/Original Draft Preparation (supporting); Writing/Review & Editing (equal). **Ove Christiansen:** Conceptualization (equal); Formal analysis (equal); Project Administration (lead); Supervision (lead); Writing/Original Draft Preparation (equal); Writing/Review & Editing (equal).

DATA AVAILABILITY

The data that support the findings of this study are available from the corresponding author upon reasonable request.

REFERENCES

- ¹T. PLÉ, N. MAUGER, O. ADJOUA, T. J. INIZAN, L. LAGARDÈRE, S. HUPPERT, and J.-P. PIQUEMAL, J. Chem. Theory Comput. **19**, 1432 (2023), Publisher: American Chemical Society.
- ²T. E. MARKLAND and M. CERIOTTI, Nat. Rev. Chem. **2**, 1 (2018), Number: 3 Publisher: Nature Publishing Group.
- ³O. CHRISTIANSEN, J. Chem. Phys. **120**, 2149 (2004).
- ⁴M. B. HANSEN, N. K. MADSEN, A. ZOCCANTE, and O. CHRISTIANSEN, J. Chem. Phys. **151**, 154116 (2019).
- ⁵N. K. MADSEN, A. B. JENSEN, M. B. HANSEN, and O. CHRISTIANSEN, J. Chem. Phys. **153**, 234109 (2020).
- ⁶J. ARPONEN, Ann Phys (N Y) **151**, 311 (1983).

- ⁷S. KVAAL, J. Chem. Phys. **136**, 194109 (2012).
- ⁸D. A. PIGG, G. HAGEN, H. NAM, and T. PAPENBROCK, Phys. Rev. C **86**, 014308 (2012).
- ⁹G. HAGEN, T. PAPENBROCK, M. HJORTH-JENSEN, and D. J. DEAN, Rep. Prog. Phys. **77**, 096302 (2014), Publisher: IOP Publishing.
- ¹⁰B. S. OFSTAD, E. AURBAKKEN, Ø. S. SCHØYEN, H. E. KRISTIANSEN, S. KVAAL, and T. B. PEDERSEN, Wiley Interdiscip. Rev. Comput. Mol. Sci. , e1666 (2023), eprint: <https://onlinelibrary.wiley.com/doi/pdf/10.1002/wcms.1666>.
- ¹¹T. B. PEDERSEN and S. KVAAL, J. Chem. Phys. **150**, 144106 (2019).
- ¹²T. SATO, H. PATHAK, Y. ORIMO, and K. L. ISHIKAWA, J. Chem. Phys. **148**, 051101 (2018).
- ¹³D. R. NASCIMENTO and A. E. DEPRINCE, J. Chem. Theory Comput. **12**, 5834 (2016).
- ¹⁴T. B. PEDERSEN, H. E. KRISTIANSEN, T. BODENSTEIN, S. KVAAL, and Ø. S. SCHØYEN, J. Chem. Theory Comput. **17**, 388 (2021).
- ¹⁵Z. WANG, B. G. PEYTON, and T. D. CRAWFORD, J. Chem. Theory Comput. **18**, 5479 (2022), Publisher: American Chemical Society.
- ¹⁶N. K. MADSEN, M. B. HANSEN, O. CHRISTIANSEN, and A. ZOCCANTE, J. Chem. Phys. **153**, 174108 (2020).
- ¹⁷M. G. HØJLUND, A. B. JENSEN, A. ZOCCANTE, and O. CHRISTIANSEN, J. Chem. Phys. **157**, 234104 (2022).
- ¹⁸M. G. HØJLUND, A. ZOCCANTE, and O. CHRISTIANSEN, J. Chem. Phys. **158**, 204104 (2023).
- ¹⁹H.-D. MEYER, U. MANTHE, and L. CEDERBAUM, Chem. Phys. Lett. **165**, 73 (1990).
- ²⁰M. BECK, A. JÄCKLE, G. WORTH, and H.-D. MEYER, Physics Reports **324**, 1 (2000).
- ²¹N. K. MADSEN, M. B. HANSEN, A. ZOCCANTE, K. MONRAD, M. B. HANSEN, and O. CHRISTIANSEN, J. Chem. Phys. **149**, 134110 (2018).
- ²²M. B. HANSEN, M. SPARTA, P. SEIDLER, O. CHRISTIANSEN, and D. TOFFOLI, J. Chem. Theory Comput. **6**, 235 (2010).
- ²³H. WANG and M. THOSS, J. Chem. Phys. **119**, 1289 (2003).
- ²⁴H. WANG and M. THOSS, J. Chem. Phys. **131**, 024114 (2009).
- ²⁵U. MANTHE, J. Chem. Phys. **128**, 164116 (2008).
- ²⁶O. VENDRELL and H.-D. MEYER, J. Chem. Phys. **134**, 044135 (2011).

- ²⁷H. WANG, J. Phys. Chem. A **119**, 7951 (2015).
- ²⁸G. A. WORTH, J. Chem. Phys. **112**, 8322 (2000).
- ²⁹R. WODRASZKA and T. CARRINGTON, J. Chem. Phys. **145**, 044110 (2016).
- ³⁰R. WODRASZKA and T. CARRINGTON, J. Chem. Phys. **146**, 194105 (2017).
- ³¹H. R. LARSSON and D. J. TANNOR, J. Chem. Phys. **147**, 044103 (2017).
- ³²N. K. MADSEN, M. B. HANSEN, G. A. WORTH, and O. CHRISTIANSEN, J. Chem. Theory Comput. **16**, 4087 (2020).
- ³³N. K. MADSEN, M. B. HANSEN, G. A. WORTH, and O. CHRISTIANSEN, J. Chem. Phys. **152**, 084101 (2020).
- ³⁴I. BURGHARDT, H. MEYER, and L. CEDERBAUM, J. Chem. Phys. **111**, 2927 (1999).
- ³⁵I. BURGHARDT, K. GIRI, and G. A. WORTH, J. Chem. Phys. **129**, 174104 (2008).
- ³⁶G. A. WORTH and I. BURGHARDT, Chem. Phys. Lett. **368**, 502 (2003).
- ³⁷G. RICHINGS, I. POLYAK, K. SPINLOVE, G. WORTH, I. BURGHARDT, and B. LASORNE, Int. Rev. Phys. Chem. **34**, 269 (2015).
- ³⁸D. V. SHALASHILIN and M. S. CHILD, J. Chem. Phys. **115**, 5367 (2001).
- ³⁹J. A. GREEN, A. GRIGOLO, M. RONTO, and D. V. SHALASHILIN, J. Chem. Phys. **144**, 024111 (2016).
- ⁴⁰B. F. E. CURCHOD and T. J. MARTÍNEZ, Chem. Rev. **118**, 3305 (2018), PMID: 29465231.
- ⁴¹S. RÖMER, M. RUCKENBAUER, and I. BURGHARDT, J. Chem. Phys. **138**, 064106 (2013), Publisher: American Institute of Physics.
- ⁴²P. EISENBRANDT, M. RUCKENBAUER, and I. BURGHARDT, J. Chem. Phys. **149**, 174102 (2018), Publisher: American Institute of Physics.
- ⁴³S. M. GREENE and V. S. BATISTA, J. Chem. Theory Comput. **13**, 4034 (2017), Publisher: American Chemical Society.
- ⁴⁴M. DUTRA, S. WICKRAMASINGHE, and S. GARASHCHUK, J. Chem. Theory Comput. **16**, 18 (2020), Publisher: American Chemical Society.
- ⁴⁵T. MURAKAMI and T. J. FRANKCOMBE, J. Chem. Phys. **149**, 134113 (2018), Publisher: American Institute of Physics.
- ⁴⁶M. A. C. SALLER and S. HABERSHON, J. Chem. Theory Comput. **13**, 3085 (2017), Publisher: American Chemical Society.
- ⁴⁷A. BAIARDI and M. REIHER, J. Chem. Theory Comput. **15**, 3481 (2019), Publisher:

American Chemical Society.

- ⁴⁸P. SEIDLER, M. B. HANSEN, and O. CHRISTIANSEN, J. Chem. Phys. **128**, 154113 (2008).
- ⁴⁹A. ZOCCANTE, P. SEIDLER, and O. CHRISTIANSEN, J. Chem. Phys. **134**, 154101 (2011).
- ⁵⁰O. CHRISTIANSEN, J. Chem. Phys. **120**, 2140 (2004).
- ⁵¹O. CHRISTIANSEN, D. G. ARTIUKHIN, I. H. GODTLIEBSEN, E. M. GRAS, W. GYÖRFFY, M. B. HANSEN, M. B. HANSEN, M. G. HØJLUND, A. B. JENSEN, N. M. HØYER, E. L. KLINTING, J. KONGSTED, C. KÖNIG, D. MADSEN, N. K. MADSEN, K. MONRAD, G. SCHMITZ, P. SEIDLER, K. SNESKOV, M. SPARTA, B. THOMSEN, D. TOFFOLI, and A. ZOCCANTE, MidasCpp.
- ⁵²M. SPARTA, D. TOFFOLI, and O. CHRISTIANSEN, Theor. Chem. Acc. **123**, 413 (2009).
- ⁵³C. BANNWARTH, S. EHLERT, and S. GRIMME, J. Chem. Theory Comput. **15**, 1652 (2019), PMID: 30741547.